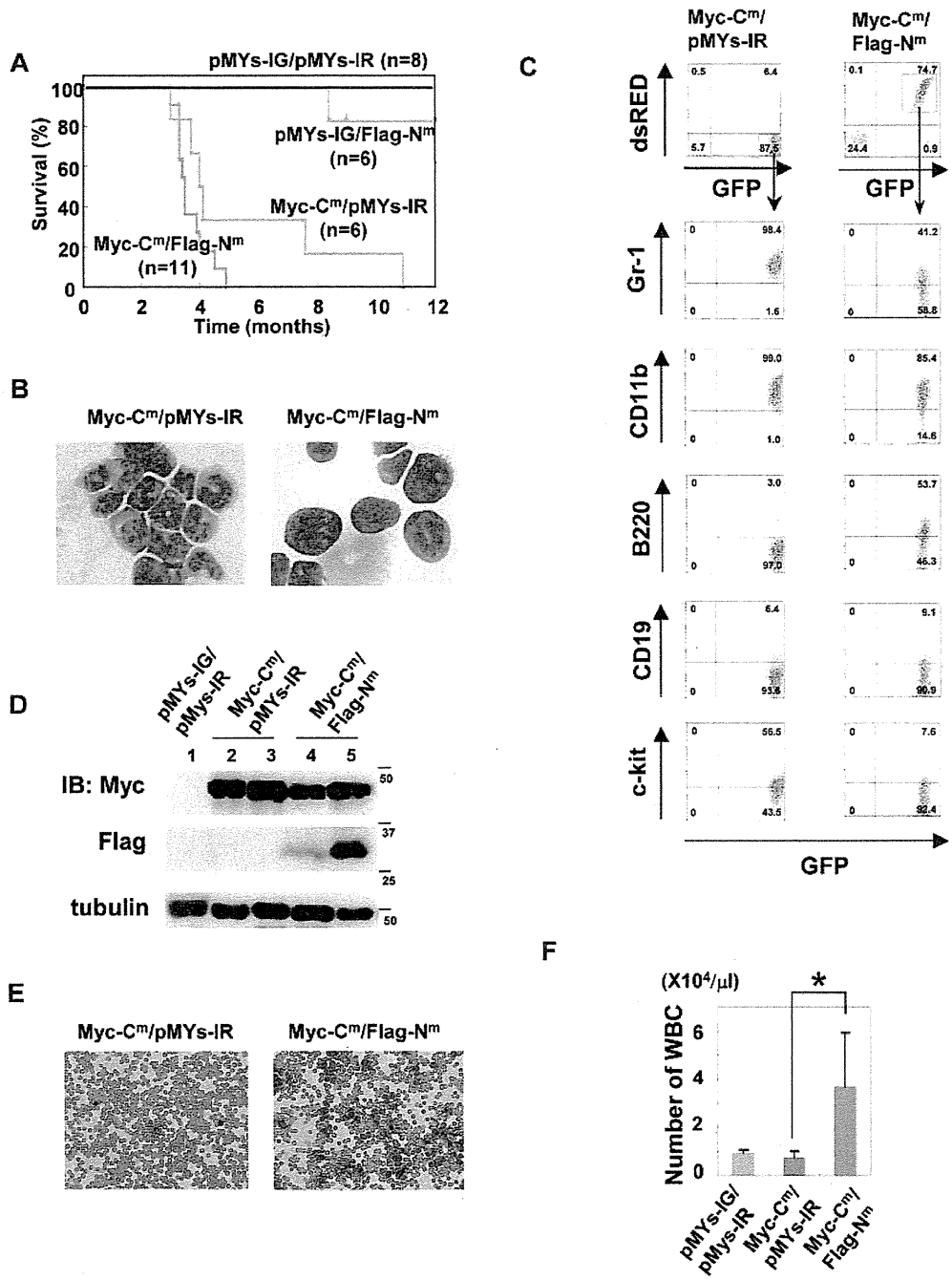

Figure 5. Coexpression of both C/EBPα-C^m and C/EBPα-N^m led to AML with leukocytosis with shorter latencies. (A) Kaplan-Meier analysis for the survival of mice that received transplants of BM cells transduced with both Myc-tagged C/EBPα-C^m-IG and pMYs-IR (Myc-C^m/pMYs-IR, n = 6), both pMYs-IG and Flag-tagged C/EBPα-N^m-IR (pMYs-IG/Flag-N^m, n = 6), both Myc-tagged C/EBPα-C^m-IG and Flag-tagged C/EBPα-N^m-IR (Myc-C^m/Flag-N^m, n = 11), or mock (pMYs-IG/pMYs-IR, n = 8). (B) Cytospin preparations of BM cells derived from mice/My-C^m/pMYs-IR or mice/Myc-C^m/Flag-N^m were stained with Giemsa. A representative photograph is shown. Images were obtained with a BX51 microscope and a DP12 camera (Olympus); objective lens, UplanFl (Olympus); original magnification ×100. (C) Flow cytometric analysis of BM cells derived from mice/Myc-C^m/pMYs-IR (left) or mice/Myc-C^m/Flag-N^m (right). The dot plots show expression of dsRED versus expression of GFP (1st panel). In the indicated gating, the dot plots show expression of Gr-1, CD11b, B220, CD19, or c-kit labeled with phycoerythrin-Cy5–conjugated streptavidin versus expression of GFP. (D) Expression of Myc-tagged C/EBPα-C^m protein and p30 protein generated by Flag-tagged C/EBPα-N^m in BM cells derived from mice/pMYs-IG/pMYs-IR (lane 1), mice/Myc-C^m/pMYs-IR (lanes 2-3), or mice/Myc-C^m/Flag-N^m (lanes 4-5) was detected by using anti-Myc monoclonal Ab (top) and ant-Flag mAb (middle), respectively, in Western blot analysis. Equal loading was evaluated by probing the immunoblots with anti-tubulin Ab (bottom). Data are representative of 3 independent experiments. (E) Peripheral blood smears obtained from mice/Myc-C^m/pMYs-IR (left) or mice/Myc-C^m/Flag-N^m (right) were stained with Giemsa. Images were obtained with a BX51 microscope and a DP12 camera (Olympus); objective lens, UplanFl (Olympus); original magnification ×20. (F) Counts of white blood cells (WBC) obtained from mice/Myc-C^m/pMYs-IR (n = 6), mice/Myc-C^m/Flag-N^m (n = 8), or mice/pMYs-IG/pMYs-IR (n = 8). All data points correspond to the mean and the standard deviation (SD). Statistically significant differences are shown. *$P < .05$.

reported that PU.1 plays important roles in macrophage differentiation, which is hampered by its interaction with C/EBPα through its C-terminal bZIP domain,[50] we investigated whether PU.1 plays some role in C/EBPα-C^m–mediated transcription. The present

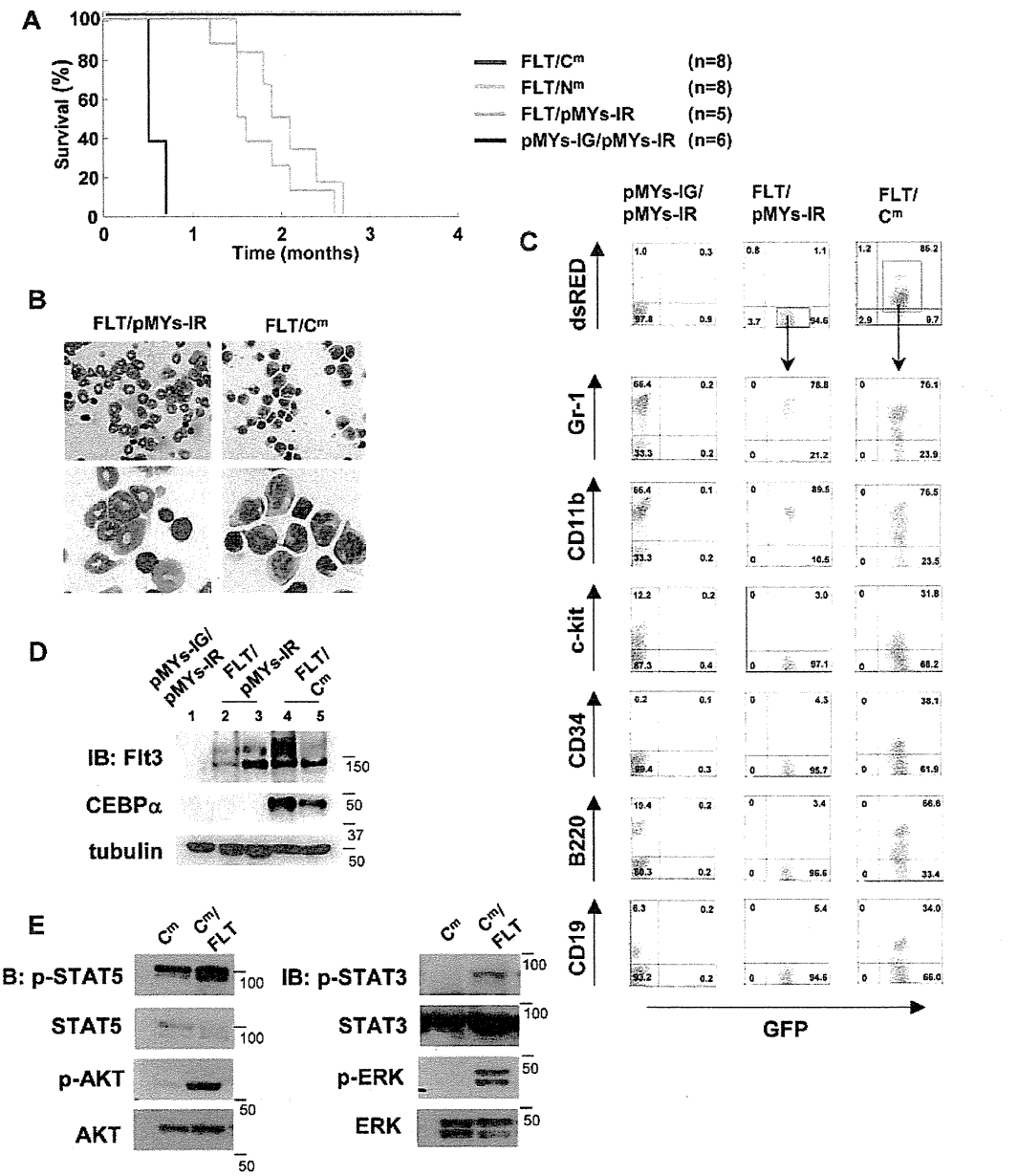

Figure 6. C/EBPα-C^m, but not C/EBPα-N^m, collaborated with Flt3-ITD in inducing aggressive AML. (A) Kaplan-Meier analysis for the survival of mice that received transplants of BM cells transduced with both Flt3-ITD-IG and pMYs-IR (FLT/pMYs-IR, n = 5), both Flt3-ITD-IG and C/EBPα-C^m-IR (FLT/C^m, n = 8), both Flt3-ITD-IG and C/EBPα-N^m-IR (FLT/N^m, n = 8), or mock (pMYs-IG/pMYs-IR, n = 8). (B) Cytospin preparations of BM cells derived from mice/FLT/pMYs-IR or mice/FLT/C^m were stained with Giemsa. Images were obtained with a BX51 microscope and a DP12 camera (Olympus); objective lens, UplanFl (Olympus); original magnification ×40 (top), ×100 (bottom). (C) Flow cytometric analysis of BM cells derived from mice/pMYs-IG/pMYs-IR, mice/FLT/pMYs-IR, or mice/FLT/C^m. The dot plots show expression of dsRED versus expression of GFP (first panel). In the indicated gating, the dot plots show expression of Gr-1, CD11b, c-kit, CD34, B220, or CD19 labeled with phycoerythrin-Cy5–conjugated streptavidin versus expression of GFP. (D) Expression of C/EBPα-C^m or Flt3-ITD in spleen cells of mice/pMYs-IG/pMYs-IR (lane 1), mice/FLT/pMYs-IG (lanes 2-3), or mice/FLT/C^m (lanes 4-5) was detected by using anti-C/EBPα (14AA) Ab (middle) or anti-Flt3 Ab (top), respectively, in Western blot analysis. Equal loading was evaluated by probing the immunoblots with anti-tubulin Ab. Data are representative of 3 independent experiments. (E) Immortalized leukemic cells derived from mice/FLT/C^m had increased phosphorylation of STAT5, AKT, STAT3, and ERK compared with those from mice/C^m. Whole-cell extracts of the former cells (immortalized in the absence of IL-3) or the latter (immortalized in the presence of IL-3) were immunoblotted with phospho-specific Abs as described in the Methods. Equal loading was evaluated by reprobing the immunoblots with anti-STAT5, anti-AKT, anti-STAT3, or anti-ERK Abs. Data are representative of 3 independent experiments.

result indicated that C/EBPα synergized with exogenously expressed PU.1 in stimulating transcription of the target genes in 293T cells, which was profoundly inhibited by C/EBPα-C^m but not by C/EBPα-N^m (Figure 2B), and suggested that C/EBPα-C^m hampers PU.1 from interacting with other molecules including C/EBPα in hemopoietic cells, leading to inhibition of granulocytic differentiation.

As for cooperation between C/EBPα-N^m and C/EBPα-C^m in leukemogenesis, we demonstrated using BMT models that C/EBPα-N^m and C/EBPα-C^m in combination induced AML with shorter latencies compared with transplantation of C/EBPα-C^m–transduced BM cells alone. In addition, combining both mutations resulted in increased number of leukemic cells, implicating C/EBPα-N^m in expansion of the cells whose differentiation was

blocked by C/EBPα-C^m. Thus, these results suggested that C/EBPα-C^m works as a class II mutation while C/EBPα-N^m works as a class I mutation in inducing leukemia.[31-36] To test this hypothesis, we built another BMT model where BM cells transduced with Flt3-ITD and either C/EBPα-C^m or C/EBPα-N^m were transplanted to lethally irradiated mice. Flt3-ITD dramatically shortened the latency of leukemia induced by C/EBPα-C^m but not by C/EBPα-N^m, indicating that C/EBPα-C^m worked as a class II mutation in inducing leukemia. Transplantation of BM cells transduced with both C/EBPα-C^m and Flt3-ITD quickly induced leukemia in just 2 weeks after transplantation. Most of the transplanted mice seemed to develop biphenotypic leukemia as assessed on the morphology and surface marker expressions (Figure 6B-C). In our hands, BM cells transduced with Flt3-ITD sometimes induce lymphoid malignancies in addition to myeloproliferative disease,[49] bringing some complexity to the experiment. Nonetheless, dramatically shortened latencies with the combination of C/EBPα-C^m and Flt3-ITD strongly indicated that C/EBPα-C^m works as a class II mutation in inducing leukemia. On the other hand, because the expression levels of C/EBPα-N^m was low in our experiments, further experiments will be required to firmly demonstrate that C/EBPα-N^m plays a class I-like role. One possible experiment is to test a combination between C/EBPα-N^m and a known class II mutation. Nonetheless, a class I-like role of C/EBPα-N^m was suggested by the marked increase in the number of leukemic cells in mice/Myc-C^m/Flag-N^m compared with mice/Myc-C^m/pMYs-IR. In relation to this, although the "2-hit theory" well explain many clinical observations, additional classes of mutations may be required for the comprehensive understanding of leukemogenesis as proposed by Renneville et al[32] In fact, we detected more than 3 mutations including mutations, chromosomal translocations, or deletions in 5 of 20 patients with leukemia and MDS (Table 1).

Concerning the in vivo effects of *CEBPA* mutations, several different results were reported.[29,30,51-54] Bereshchenko et al[30] have recently published a report using knock-in mice that C/EBPα-p30 and a C-terminal mutation collaborated in inducing leukemia. Our results basically agreed with those by Bereshchenko et al. However, while our results implicated C-terminal mutations of C/EBPα in differentiation, leading to leukemia with relatively long latencies, Bereshchenko et al[30] suggested premalignant HSC expansion by C-terminal mutations. The reason for the disparity is not clear, but was partly caused by the difference in the strength or functions of different C-terminal mutants or in the expression levels of mutants in knock-in mice and BMT models. Concerning the experimental systems, knock-in mice are superior to mouse BMT models in several aspects as indicated previously.[29,30] Most importantly, expression of the mutant C/EBPα is driven by the authentic promoter in knock-in mice while it is over-driven by an external promoter in BMT models. Moreover, replacement of both alleles with different C/EBPα mutations closely mimics human leukemia, as it lacks the WT C/EBPα unlike the BMT model. In addition, in BMT models, retrovirus integration sites sometimes modify the phenotype of the disease. However, BMT models do have some advantages. First, in contrast to knock-in mice where all hemopoietic cells express the mutant allele, only some cells can be of a leukemia origin, which would more faithfully mimic human pathologic situations. In addition, various mutants can be readily tested in vivo. Bereshchenko et al[30] used K313dup as a C-terminal *CEBPA* mutation, demonstrating that mice$^{K313dup/+}$ did not develop leukemia. K313dup was a weak inducer of leukemia in our BMT model, where only 1 of the 4 transplanted mice developed myeloid leukemia in 10 months (data not shown). On the other hand, C/EBPα-C^m, a C-terminal mutation with 304-323dup that we used in the present study, induced leukemia in most transplanted mice (Figure 4A). Thus, knock-in mice models and BMT models can complement with each other in investigating in vivo leukemogenesis.

To summarize, we have presented a series of evidence, including clinical data, in vitro experiments, and mouse BMT models, showing that 2 different mutations of *CEBPA*, C/EBPα-N^m and C/EBPα-C^m, play distinct roles in leukemogenesis. Moreover, our results strongly indicated that C/EBPα-C^m is able to play as a class II mutation in concert with Flt3-ITD in inducing leukemia. Further elucidation of the molecular mechanism of *CEBPA* mutations–induced leukemia may pave a novel way to treating patients with leukemia.

Acknowledgments

We thank Dr Atsushi Iwama, Dr Claus Nerlov, and Dr Shigekazu Nagata for kindly providing plasmids. We are grateful to Dr Dovie Wylie for her excellent editing of the English.

This work was supported by the Ministry of Education, Science, Technology, Sports and Culture, Japan and in part supported by Global COE Program "Center of Education and Research for the Advanced Genome-Based Medicine, for personalized medicine and the control of worldwide infectious diseases," MEXT, Japan.

Authorship

Contribution: N.K. did all the experiments and participated in writing the manuscript; J.K. oversaw all the experiments and actively participated in manuscript writing; N.D., Y.K., N.W.O., K.T., F.N., T.O., and Y.E. technically supported BMT; Y.F. and H.N. provided plasmids and reagents; Y.H. and H.H. provided and analyzed human samples; and T.K. conceived the project, secured funding, and actively participated in manuscript writing.

Conflict-of-interest disclosure: T.K. serves as a consultant for R&D Systems. The remaining authors declare no competing financial interests.

Correspondence: Toshio Kitamura, Division of Cellular Therapy and Division of Stem Cell Signaling, The Institute of Medical Science, The University of Tokyo, 4-6-1 Shirokanedai, Minato-ku, Tokyo 108-8639, Japan; e-mail: kitamura@ims.u-tokyo.ac.jp.

References

1. Zhang P, Iwasaki-Arai J, Iwasaki H, et al. Enhancement of hematopoietic stem cell repopulating capacity and self-renewal in the absence of the transcription factor C/EBP alpha. *Immunity.* 2004;21(6):853-863.
2. Tenen DG, Hromas R, Licht JD, Zhang D-E. Transcription factors, normal myeloid development, and leukemia. *Blood.* 1997;90(2):489-519.
3. Friedman AD, McKnight SL. Identification of two polypeptide segments of CCAAT/enhancer-binding protein required for transcriptional activation of the serum albumin gene. *Genes Dev.* 1990;4(8):1416-1426.
4. Landschulz WH, Johnson PF, McKnight SL. The DNA binding domain of the rat liver nuclear protein C/EBP is bipartite. *Science.* 1989;243(4899):1681-1688.
5. Nerlov C, Ziff EB. CCAAT/enhancer binding protein-alpha amino acid motifs with dual TBP and TFIIB binding ability co-operate to activate transcription in both yeast and mammalian cells. *Embo J.* 1995;14(17):4318-4328.
6. Lin FT, MacDougald OA, Diehl AM, Lane MD. A 30-kDa alternative translation product of the CCAAT/enhancer binding protein alpha message:

transcriptional activator lacking antimitotic activity. *Proc Natl Acad Sci U S A.* 1993;90(20):9606-9610.

7. Calkhoven CF, Muller C, Leutz A. Translational control of C/EBPalpha and C/EBPbeta isoform expression. *Genes Dev.* 2000;14(15):1920-1932.
8. Pabst T, Mueller BU, Zhang P, et al. Dominant-negative mutations of CEBPA, encoding CCAAT/enhancer binding protein-alpha (C/EBPalpha), in acute myeloid leukemia. *Nat Genet.* 2001;27(3):263-270.
9. Radomska HS, Huettner CS, Zhang P, Cheng T, Scadden DT, Tenen DG. CCAAT/enhancer binding protein alpha is a regulatory switch sufficient for induction of granulocytic development from bipotential myeloid progenitors. *Mol Cell Biol.* 1998;18(7):4301-4314.
10. Christy RJ, Yang VW, Ntambi JM, et al. Differentiation-induced gene expression in 3T3-L1 preadipocytes: CCAAT/enhancer binding protein interacts with and activates the promoters of two adipocyte-specific genes. *Genes Dev.* 1989;3(9):1323-1335.
11. McNagny KM, Sieweke MH, Doderlein G, Graf T, Nerlov C. Regulation of eosinophil-specific gene expression by a C/EBP-Ets complex and GATA-1. *Embo J.* 1998;17(13):3669-3680.
12. Umek RM, Friedman AD, McKnight SL. CCAAT-enhancer binding protein: a component of a differentiation switch. *Science.* 1991;251(4991):288-292.
13. Slomiany BA, D'Arigo KL, Kelly MM, Kurtz DT. C/EBPalpha inhibits cell growth via direct repression of E2F-DP-mediated transcription. *Mol Cell Biol.* 2000;20(16):5986-5997.
14. Porse BT, Bryder D, Theilgaard-Monch K, et al. Loss of C/EBP alpha cell cycle control increases myeloid progenitor proliferation and transforms the neutrophil granulocyte lineage. *J Exp Med.* 2005;202(1):85-96.
15. Porse BT, Pedersen TA, Xu X, et al. E2F repression by C/EBPalpha is required for adipogenesis and granulopoiesis in vivo. *Cell.* 2001;107(2):247-258.
16. Zada AA, Pulikkan JA, Bararia D, et al. Proteomic discovery of Max as a novel interacting partner of C/EBPalpha: a Myc/Max/Mad link. *Leukemia.* 2006;20(12):2137-2146.
17. Pedersen TA, Kowenz-Leutz E, Leutz A, Nerlov C. Cooperation between C/EBPalpha TBP/TFIIB and SWI/SNF recruiting domains is required for adipocyte differentiation. *Genes Dev.* 2001;15(23):3208-3216.
18. Johansen LM, Iwama A, Lodie TA, et al. c-Myc is a critical target for c/EBPalpha in granulopoiesis. *Mol Cell Biol.* 2001;21(11):3789-3806.
19. D'Alo F, Johansen LM, Nelson EA, et al. The amino terminal and E2F interaction domains are critical for C/EBP alpha-mediated induction of granulopoietic development of hematopoietic cells. *Blood.* 2003;102(9):3163-3171.
20. Gombart AF, Hofmann WK, Kawano S, et al. Mutations in the gene encoding the transcription factor CCAAT/enhancer binding protein alpha in myelodysplastic syndromes and acute myeloid leukemias. *Blood.* 2002;99(4):1332-1340.
21. Snaddon J, Smith ML, Neat M, et al. Mutations of CEBPA in acute myeloid leukemia FAB types M1 and M2. *Genes Chromosomes Cancer.* 2003;37(1):72-78.
22. Renneville A, Boissel N, Gachard N, et al. The favorable impact of CEBPA mutations in patients with acute myeloid leukemia is only observed in the absence of associated cytogenetic abnormalities and FLT3 internal duplication. *Blood.* 2009;113(21):5090-5093.
23. Leroy H, Roumier C, Huyghe P, Biggio V, Fenaux P, Preudhomme C. CEBPA point mutations in hematological malignancies. *Leukemia.* 2005;19(3):329-334.
24. Shih LY, Liang DC, Huang CF, et al. AML patients with CEBPalpha mutations mostly retain identical mutant patterns but frequently change in allelic distribution at relapse: a comparative analysis on paired diagnosis and relapse samples. *Leukemia.* 2006;20(4):604-609.
25. Preudhomme C, Sagot C, Boissel N, et al. Favorable prognostic significance of CEBPA mutations in patients with de novo acute myeloid leukemia: a study from the Acute Leukemia French Association (ALFA). *Blood.* 2002;100(8):2717-2723.
26. Wouters BJ, Lowenberg B, Erpelinck-Verschueren CA, van Putten WL, Valk PJ, Delwel R. Double CEBPA mutations, but not single CEBPA mutations, define a subgroup of acute myeloid leukemia with a distinctive gene expression profile that is uniquely associated with a favorable outcome. *Blood.* 2009;113(13):3088-3091.
27. Fuchs O, Provaznikova D, Kocova M, et al. CEBPA polymorphisms and mutations in patients with acute myeloid leukemia, myelodysplastic syndrome, multiple myeloma and non-Hodgkin's lymphoma. *Blood Cells Mol Dis.* 2008;40(3):401-405.
28. Shih LY, Huang CF, Lin TL, et al. Heterogeneous patterns of CEBPalpha mutation status in the progression of myelodysplastic syndrome and chronic myelomonocytic leukemia to acute myelogenous leukemia. *Clin Cancer Res.* 2005;11(5):1821-1826.
29. Kirstetter P, Schuster MB, Bereshchenko O, et al. Modeling of C/EBPalpha mutant acute myeloid leukemia reveals a common expression signature of committed myeloid leukemia-initiating cells. *Cancer Cell.* 2008;13(4):299-310.
30. Bereshchenko O, Mancini E, Moore S, et al. Hematopoietic stem cell expansion precedes the generation of committed myeloid leukemia-initiating cells in C/EBPalpha mutant AML. *Cancer Cell.* 2009;16(5):390-400.
31. Dash A, Gilliland DG. Molecular genetics of acute myeloid leukaemia. *Best Pract Res Clin Haematol.* 2001;14(1):49-64.
32. Renneville A, Roumier C, Biggio V, et al. Cooperating gene mutations in acute myeloid leukemia: a review of the literature. *Leukemia.* 2008;22(5):915-931.
33. Kottaridis PD, Gale RE, Frew ME, et al. The presence of a FLT3 internal tandem duplication in patients with acute myeloid leukemia (AML) adds important prognostic information to cytogenetic risk group and response to the first cycle of chemotherapy: analysis of 854 patients from the United Kingdom Medical Research Council AML 10 and 12 trials. *Blood.* 2001;98(6):1752-1759.
34. Beghini A, Ripamonti CB, Cairoli R, et al. KIT activating mutations: incidence in adult and pediatric acute myeloid leukemia, and identification of an internal tandem duplication. *Haematologica.* 2004;89(8):920-925.
35. Ono R, Nakajima H, Ozaki K, et al. Dimerization of MLL fusion proteins and FLT3 activation synergize to induce multiple-lineage leukemogenesis. *J Clin Invest.* 2005;115(4):919-929.
36. Kelly LM, Kutok JL, Williams IR, et al. PML/RARalpha and FLT3-ITD induce an APL-like disease in a mouse model. *Proc Natl Acad Sci U S A.* 2002;99(12):8283-8288.
37. Ding Y, Harada Y, Imagawa J, Kimura A, Harada H. AML1/RUNX1 point mutation possibly promotes leukemic transformation in myeloproliferative neoplasms. *Blood.* 2009;114(25):5201-5205.
38. Yokota S, Kiyoi H, Nakao M, et al. Internal tandem duplication of the FLT3 gene is preferentially seen in acute myeloid leukemia and myelodysplastic syndrome among various hematological malignancies. A study on a large series of patients and cell lines. *Leukemia.* 1997;11(10):1605-1609.
39. Murata K, Kumagai H, Kawashima T, et al. Selective cytotoxic mechanism of GTP-14564, a novel tyrosine kinase inhibitor in leukemia cells expressing a constitutively active Fms-like tyrosine kinase 3 (FLT3). *J Biol Chem.* 2003;278(35):32892-32898.
40. Watanabe-Okochi N, Kitaura J, Ono R, et al. AML1 mutations induced MDS and MDS/AML in a mouse BMT model. *Blood.* 2008;111(8):4297-4308.
41. Morita S, Kojima T, Kitamura T. Plat-E: an efficient and stable system for transient packaging of retroviruses. *Gene Ther.* 2000;7(12):1063-1066.
42. Kitamura T, Koshino Y, Shibata F, et al. Retrovirus-mediated gene transfer and expression cloning: powerful tools in functional genomics. *Exp Hematol.* 2003;31(11):1007-1014.
43. Lu Y, Kitaura J, Oki T, et al. Identification of TSC-22 as a potential tumor suppressor that is upregulated by Flt3-D835V but not Flt3-ITD. *Leukemia.* 2007;21(11):2246-2257.
44. Fukuchi Y, Shibata F, Ito M, et al. Comprehensive analysis of myeloid lineage conversion using mice expressing an inducible form of C/EBP alpha. *EMBO J.* 2006;25(14):3398-3410.
45. Cleaves R, Wang QF, Friedman AD. C/EBPalphap30, a myeloid leukemia oncoprotein, limits G-CSF receptor expression but not terminal granulopoiesis via site-selective inhibition of C/EBP DNA binding. *Oncogene.* 2004;23(3):716-725.
46. Wang QF, Friedman AD. CCAAT/enhancer-binding proteins are required for granulopoiesis independent of their induction of the granulocyte colony-stimulating factor receptor. *Blood.* 2002;99(8):2776-2785.
47. Iwasaki M, Kuwata T, Yamazaki Y, et al. Identification of cooperative genes for NUP98-HOXA9 in myeloid leukemogenesis using a mouse model. *Blood.* 2005;105(2):784-793.
48. Hasemann MS, Damgaard I, Schuster MB, et al. Mutation of C/EBPalpha predisposes to the development of myeloid leukemia in a retroviral insertional mutagenesis screen. *Blood.* 2008;111(8):4309-21.
49. Nakajima H, Shibata F, Kumagai H, Shimoda K, Kitamura T. Tyk2 is dispensable for induction of myeloproliferative disease by mutant FLT3. *Int J Hematol.* 2006;84(1):54-59.
50. Reddy VA, Iwama A, Iotzova G, et al. Granulocyte inducer C/EBPalpha inactivates the myeloid master regulator PU. 1: possible role in lineage commitment decisions. *Blood.* 2002;100(2):483-490.
51. Schwieger M, Löhler J, Fischer M, Herwig U, Tenen DG, Stocking C. A dominant-negative mutant of C/EBPalpha, associated with acute myeloid leukemias, inhibits differentiation of myeloid and erythroid progenitors of man but not mouse. *Blood.* 2004;103(7):2744-2752.
52. Iwama A, Osawa M, Hirasawa R, et al. Reciprocal roles for CCAAT/enhancer binding protein (C/EBP) and PU. 1 transcription factors in Langerhans cell commitment. *J Exp Med.* 2002;195(5):547-558.
53. Nerlov C. C/EBPalpha mutations in acute myeloid leukaemias. *Nat Rev Cancer.* 2004;4(5):394-400.
54. Schuster MB, Porse BT. C/EBPalpha: a tumour suppressor in multiple tissues? *Biochim Biophys Acta.* 2006;1766(1):88-103.

Expression of ADAMTS4 in Ewing's sarcoma

K. MINOBE[1,2], R. ONO[1*], A. MATSUMINE[3*], F. SHIBATA-MINOSHIMA[2], K. IZAWA[2], T. OKI[2], J. KITAURA[2], T. IINO[3], J. TAKITA[4], S. IWAMOTO[5], H. HORI[5], Y. KOMADA[5], A. UCHIDA[3], Y. HAYASHI[6], T. KITAMURA[2] and T. NOSAKA[1]

[1]Department of Microbiology and Molecular Genetics, Mie University Graduate School of Medicine, Tsu; [2]Division of Cellular Therapy, The Institute of Medical Science, The University of Tokyo, Tokyo; [3]Department of Orthopaedic Surgery, Mie University Graduate School of Medicine, Tsu; [4]Department of Cell Therapy and Transplantation Medicine, Graduate School of Medicine, The University of Tokyo, Tokyo; [5]Department of Pediatrics and Developmental Science, Mie University Graduate School of Medicine, Tsu; [6]Gunma Children's Medical Center, Gunma, Japan

Received March 29, 2010; Accepted May 18, 2010

DOI: 10.3892/ijo_00000706

Abstract. Ewing's sarcoma (EWS) is a malignant bone tumor that frequently occurs in teenagers. Genetic mutations which cause EWS have been investigated, and the most frequent one proved to be a fusion gene between *EWS* gene of chromosome 22 and the *FLI1* gene of chromosome 11. However, a limited numbers of useful biological markers for diagnosis of EWS are available. In this study, we identified ADAMTS4 (a disintegrin and metalloproteinase with thrombospondin motifs) as a possible tumor marker for EWS using the retrovirus-mediated signal sequence trap method. ADAMTS4 is a secreted protein of 837 amino acids with a predicted molecular mass of 98-100 kDa. It is a member of metalloprotease family, is expressed mainly in cartilage and brain, and regulates the degradation of aggrecans. ADAMTS4 has been suggested to be involved in arthritic diseases and gliomas. Herein, we show that *ADAMTS4* mRNA was expressed in all primary EWS samples and all EWS-derived cell lines examined, while its expression was detected only in small subpopulations of other solid tumors. Furthermore, *ADAMTS4* expression was found to be regulated by *EWS-FLI1* fusion gene-dependent manner. We also demonstrated that ADAMTS4 protein was highly expressed in tumor samples of the patients with EWS by using immunohistochemistry. These results suggest that ADAMTS4 is a novel tumor marker for EWS.

Correspondence to: Dr T. Nosaka, Department of Microbiology and Molecular Genetics, Mie University Graduate School of Medicine, 2-174, Edobashi, Tsu 514-8507, Japan
E-mail: nosaka@doc.medic.mie-u.ac.jp

*Contributed equally

Key words: EWS-FLI1, tumor marker, signal sequence trap, retrovirus

Introduction

Ewing's sarcoma (EWS) is the second most frequent primary bone tumor of childhood and adolescence with aggressive clinical course and poor prognosis. It is recognized that EWS is a part of Ewing's sarcoma family of tumors (ESFTs) which also include the peripheral primitive neuroectodermal tumor (PNET) (1,2), Askin's tumor and extraosseous EWS. Biologically, ESFTs are characterized by common chromosomal translocation between the 5' portion of the *EWS* gene (22q12) and the 3' portion of the members of the *ETS* family genes (3). More than 85% of the cases have the fusion gene *EWS-FLI1* due to t(11;22)(q24;q12) (4,5). Five to 10% of the cases pocess *EWS-ERG* due to t(21;22)(q22;q12) (6). The other rare cases are *EWS-ETV1*, *EWS-E1AF* and *EWS-FEV*, each resulting from t(7;22)(p22;q12), t(17;22) (q12;q12) and t(2;22)(q33;q12), respectively (3,7,8). The EWS-ETS chimeric proteins behave as aberrant transcriptional regulators and are believed to play a crucial role in the onset and progression of the ESFTs (9,10).

Currently, diagnosis of EWS is determined mainly by CD99 immunohistochemistry (11-13), and by genetic aberration. However, CD99 expression is also reported to be positive in some T cell acute lymphoblastic leukemia (T-ALL), acute myelogenous leukemia (AML), ependymoma, synovial sarcoma and pancreatic endocrine tumors (14-16). Besides, not all EWSs have this specific chromosomal translocation. Thus, there is no specific biomarker for differentiating EWS from other soft tissue sarcomas. Among the patients with localized tumor at diagnosis, 20% relapse within 4 years and die of the disease. In contrast, 5-year survival rate is ~20-30% in cases with metastasis. This study was performed to find a useful tumor marker for EWS.

The signal sequence trap (SST) is a strategy to identify complementary DNAs (cDNAs) containing signal sequence that encode secreted and type I membrane proteins (17). To date, various important molecules have been detected including *SDF-1*, a member of the tumor necrosis factor receptor superfamily *TROY*, *Xenopus-Tsukushi*, *Vasorin* and leukocyte mono-Ig-like receptor (*LMIR*) by the SST method

(18-23). In this study, we identified a secreted molecule *ADAMTS4* (a disintegrin and metalloproteinase with thrombospondin motifs) from EWS cell lines by using the SST system based on retrovirus-mediated expression screening (SST-REX) (24,25).

ADAMTS is a family of proteinases which was first described in 1997 (26). Today, 19 different members of the *ADAMTS* family have been identified, but the functions, mechanisms of activation, and substrates of most members remain incompletely understood (27). Members of the *ADAMTS* family are closely related to the *ADAM* (a disintegrin and metalloproteinase) family, but unlike *ADAMs*, the *ADAMTSs* are secreted molecules, some of which bind to the extracellular matrix. *ADAMTS4* was originally purified from chondrocytes and synovial cells stimulated with interleukin-1 (28). The structure of ADAMTS4 consists of six domains, a prodomain, a metalloproteinase domain, a disintegrin domain, a thrombospondin type I motif, a cysteine-rich domain and a spacer domain. It has been demonstrated to cleave the aggrecan at Glu^{373}-Ala^{374}, and therefore is also named as *aggrecanase1* (29-32). The aggrecanase activity of ADAMTS4 is inhibited by TIMP-3 (tissue inhibitor of metalloproteinase-3) (33), which was originally identified as an inhibitor of matrix metalloproteinases. Yamanishi *et al* demonstrated that *ADAMTS4* was overexpressed in synovial cells and chondrocytes in the patients with osteoarthritis (OA) and rheumatoid arthritis (RA) (34). Thus, *ADAMTS4* is considered to play an important role in the aggrecan degradation of articular cartilage in OA and RA. Recent studies reported that ADAMTS4 cleaves not only aggrecan but also brevican, versican and α2-macroglobulin (35).

In this study, we have disclosed that *ADAMTS4* mRNA was expressed in all tissue samples of EWS patients and all EWS cell lines examined, and the mRNA level of *ADAMTS4* was regulated by *EWS-FLI1* in the cell line. We have also demonstrated the ADAMTS4 protein expression by immunostaining of the patients' samples and the cell lines. Thus, we propose that ADAMTS4 is a possible tumor marker of EWS.

Materials and methods

Cell lines. Osteosarcoma cell lines (MG63, HOS, KHOS/NP, SaOS2 and U2OS), neuroblastoma cell lines (KPNSI-FA, LAN-1 and NB69), a lung cancer cell line H460, a liver cancer cell line PLC/PRF/5, a cholangiocarcinoma cell line HuCCT1, a colon cancer cell line SW-48, T-ALL cell lines (Jurkat, PEER, CEM and HPB-ALL), B-ALL cell lines (NALM16, NALM24 and IM9), AML cell lines (MOLM13 and ML1), an acute myelomonocytic leukemia cell line U937, EWS cell lines (SJES-2, SJES-3, SJES-5, SJES-6, SJES-7 and SJES-8), rhabdomyosarcoma cell lines (RMS and SJRH-30), pancreatic cancer cell lines (AsPC-1, BxPC-3 and Capan-1), glioblastoma cell lines (U87MG, U251 and T98G), and gastric cancer cell lines (HGC-27, MKN45, GCIY and KATO-III) were cultured in RPMI-1640 medium (Sigma-Aldrich, St. Louis, MO, USA) containing 10% heat-inactivated fetal bovine serum (FBS) (Sigma-Aldrich). A murine pro-B cell line Ba/F3 was maintained in RPMI-1640 containing 10% FBS and 1 ng/ml murine interleukin-3 (IL-3) (R&D Systems, Minneapolis, MN, USA). A retrovirus packaging cell line Plat-E (36) and NIH3T3 were cultured in Dulbecco's modified Eagle's medium (DMEM) (Sigma-Aldrich) containing 10% FBS. Human mesenchymal stem/progenitor cells (hMSCs) were purchased from Sanko Junyaku (Tokyo, Japan).

Patient samples and normal controls. Samples from 7 patients with EWS, 13 osteosarcoma, 4 chondrosarcoma, 4 synovial sarcoma, and 3 rhabdomyosarcoma, which were obtained at initial surgery at the department of orthopaedic surgery at Mie University Hospital, were examined by reverse transcription (RT)-PCR. Schwannoma, desmoid and lipoma samples were used as controls. Tissue samples for immunohistochemical staining were obtained from 25 EWS patients who underwent an open biopsy or a surgical resection. For enzyme-linked immunosorbent assay (ELISA), we used serum samples of 3 osteosarcomas, 1 osteofibrous dysplasia, 1 chondrosarcoma, 1 synovial sarcoma, 6 EWS and 4 healthy volunteers. Basically sera were isolated before the chemotherapy except for few cases. Informed consent was obtained from each patient or parent and volunteer. This study was approved by the ethics committee at Mie University.

Antibodies and other reagents. A rabbit polyclonal anti-ADAMTS4 antibody which was raised against amino acids 764-837 of human ADAMTS4 (Santa Cruz Biotechnology, Santa Cruz, CA, USA) and a horseradish peroxidase (HRP)-conjugated goat anti-rabbit IgG secondary antibody (Bio-Rad Laboratories, Hercules, CA, USA) were used for immunoprecipitation (IP)-Western blot analysis. Immunostaining was performed by using the following antibodies: the same anti-ADAMTS4 antibody as used for IP-Western analysis, an N-universal rabbit IgG (Dako, Kyoto, Japan), an HRP-conjugated anti-rabbit IgG antibody (Nichirei Biosciences, Tokyo, Japan) for immunohistochemistry, and an Alexa488-conjugated anti-rabbit IgG antibody (Invitrogen, Carlsbad, CA, USA) for immunofluorescence microscopy. For ELISA, a monoclonal anti-ADAMTS4 antibody raised against amino acids 213-685 of the recombinant human ADAMTS4 (R&D Systems), a biotinylated goat anti-ADAMTS4 antibody raised against amino acids 213-685 of the recombinant human ADAMTS4 and an Avidin-HRP (eBioscience, San Diego, CA, USA) were used.

Screening of EWS cDNA library by SST. A human EWS cDNA library was screened by SST-REX as previously described (24,25). Briefly, poly(A)$^+$ RNA was prepared from EWS cell lines using the FastTrack2.0 Kit (Invitrogen). The cDNA was synthesized from the mixture of poly(A)$^+$ RNAs of 6 EWS cell lines with random hexamers, using the SuperScript Choice System (Invitrogen) according to the manufacturer's instructions. The synthesized cDNA was size-separated by electrophoresis on an agarose gel. Fractions greater than 500 bp were collected and inserted into *Bst*XI sites of pMX-SST (25) using *Bst*XI adaptors (Invitrogen). Ba/F3 cells were infected with the retroviruses expressing the EWS-derived cDNA library and selected for growth in the absence of IL-3. Genomic DNAs extracted from IL-3-independent clones were subjected to PCR to recover the

Table I. Primer sequences used in RT-PCR analyses in murine tissues.

Gene	Sense	Antisense
DKFZP56400823	5'-CCATTGCCTGTCTCTCTCATGACA-3'	5'-GAGCTGTGCTCTTCTGTTGGTGA-3'
ADAMTS4	5'-GAGCTGTGCTCTTCTGTTGGTGA-3'	5'-CAGAGAAGCGAAGCGCTTGGTT-3'
DNER	5'-GACATAATCCTGCCCCGCTCT-3'	5'-CTCTGATGGCTTCGTGGCACAT-3'
NGFR	5'-CGTGTTCTCCTGCCAGGACAA-3'	5'-GCTGTGCAGTTTCTCTCCCTCT-3'
LRRN6A	5'-GTCTTCACCGGCCTCAGCAA-3'	5'-CCCTCGATTGTACCGATTGGGTT-3'
ECSM2	5'-GACAACTCAGACCTCGCAGGAA-3'	5'-CATTGGCTGTGGAGCAGCTTTCA-3'
LGALS3BP	5'-CAGGACTACTGTGGACGGCTT-3'	5'-CTACTCCAGGTGGAAGAGGTGTA-3'
PTPRF	5'-GCTGGCCCAGGAGAAGAGTT-3'	5'-GCTCTGCCCATTGTACAGGATCTT-3'
FCGRT	5'-GCTGTGAACTGGCCTCGGATA-3'	5'-CCAGCAATGACCATGCGTGGAA-3'
LAMP2	5'-CGCTGTCTCTTGGGCTGTGAAT-3'	5'-GGCACCTTCTCCTCAGTGATGTT-3'
RCN1	5'-CTAAGCCCGGACGAGAGCAA-3'	5'-GGCCATTGTCCTCGTGGGAA-3'
MMP14	5'-CATGAGTTGGGGCATGCCCTA-3'	5'-CGGCCAAGCTCCTTAATGTGCTT-3'
SDC2	5'-CTCCATTGAGGAAGCTTCAGGAGT-3'	5'-CTTCTGGTAAGCTGCGCTGGAT-3'
DAG1	5'-GGAAGCCCACGGTCACCATT-3'	5'-GCTTGAGCTTGTCGGTAGTGGTA-3'
EPCR	5'-GGCAACGCCTCTCTGGGAAAA-3'	5'-CGGCCACACCAGCGATTATGAA-3'
CD97	5'-CTGGAACAAAGCCTTCGGACCTT-3'	5'-GTCGGTGTCCCAGTACCCATT-3'
CD99L2	5'-GTCCAGAGAGGATATGGAGACACA-3'	5'-GGTTCTGCAGACTGCGTTTCTTG-3'
IGFBP5	5'-GCGACGAGAAAGCTCTGTCCAT-3'	5'-GCCTTGTTCGGATTCCTGTCTCA-3'
CLU	5'-GAAGGCATTCCCGGAAGTGTGTA-3'	5'-GCTGGACATCCATGGCCTGTT-3'
LSAMP	5'-GCTCTGGAATACAGCCTCCGAA-3'	5'-GTGTCATCCCGGTACCACTCAA-3'
NPTN	5'-GTAACCTCACTTCCAGCTCTCACA-3'	5'-GGAGGCAGAGCCAATGGAGTT-3'
EFNA5	5'-GCAGCAACCCCAGATTCCAGA-3'	5'-GATGGCTCGGCTGACTCATGTA-3'
PODXL	5'-CCTTCACCAGTAGCAGTGGACAA-3'	5'-CCACTGTAGACGCCATAGACTGT-3'
TMEM123	5'-CCACTCAGTGCTGACCTCCAA-3'	5'-GTTCGTCAATGCTTCGGTACCGAA-3'
GAPDH	5'-CAGTATGACTCCACTCACGGCAA-3'	5'-CAGATCCACGACGGACACATTG-3'

integrated cDNAs using vector primers. The resulting PCR fragments were sequenced and analyzed.

RT-PCR analysis. RT-PCR was carried out to detect *ADAMTS4* transcript in tumor cell lines, murine tissues and patients' samples. Total RNA was isolated with acid guanidium-phenol-chloroform method, and then 5 μg RNA was reverse-transcribed to cDNA in a total volume of 33 μl with random hexamers by using the Ready-To-Go You-Prime First-Strand Beads (GE Healthcare UK, Buckinghamshire, UK). RT-PCR was performed with the programmable cyclic reactor under the following conditions: denaturation at 94°C for 3 min followed by 30 cycles of amplification (94°C for 30 sec, 60°C for 30 sec, and 72°C for 45 sec). PCR product was separated by 1-2% agarose gel electrophoresis and visualized by ethidium bromide staining. The primers used for RT-PCR was described in Tables I and II.

Cloning of the full-length cDNA encoding ADAMTS4. Full-length *ADAMTS4* was generated as follows. The first half of *ADAMTS4* (1-1194 bp) was isolated from pMX-SST vector by digestion with *Bam*HI. Based on the sequence data, the last half (1195-2514 bp) were amplified by PCR from cDNAs of the EWS cell line SJES-5, and digested with *Bam*HI and *Not*I. The fragment was subcloned into a pMXs-puro retroviral vector (37). The resultant vector was digested with *Bam*HI, and then ligated with the *Bam*HI fragment of the first half of *ADAMTS4*. The primers used for amplification are as follows: SST5', 5'-GGGGGTGGACCATCCTCTA-3'; SST3', 5'-CGCGCAGCTGTAAACGGTAG-3'; ADAMTS4-FL-S, 5'-GAAAGAATTCGCTGCAGTACCAGTGCCATG-3'; ADAMTS4-FL-S2, 5'-GAGCACCTCTCGCCATGTCA-3'; ADAMTS4-FL-AS, 5'-GAAAGAGAATTCGCGGCC GCTTATTTCCTGCCCGCCCAGG-3'; ADAMTS4-AS2, 5'-CTTTGGATCCACATGAGCCATCACAGGGGCCA TGACATGGCGAGAGGTGCTCAAAGGCCCATTCAAA CTGATGCATG-3'.

Transfection and infection. Retroviral transfection was done as described previously (36,37). Briefly, retroviruses were generated by transient transfection of Plat-E packaging cells (36) with FuGENE 6 (Roche Diagnostics, Basel, Switzerland). Ba/F3 and NIH3T3 cells were infected with the retroviruses in the presence of 10 μg/ml polybrene. Selection with G418 or puromycin was started 48 h after infection.

Small interfering (si)RNA design and transfection experiments. *EWS-FLI1*-specific siRNA (siEF1) for SJES-5 cell line was designed as previously described (38). As a negative control, siGFP was employed (Hayashi-Kasei, Osaka, Japan).

Table II. Primer sequences used in RT-PCR analyses in human cancer cell lines.

Gene	Sense	Antisense
DKFZP56400823	5'-CCATCTGGACTAGCTCTCCACA-3'	5'-GTGCTGGTCACAGTGGAGCTA-3'
ADAMTS4	5'-GTGGAGTCTCCACTTGCGACA-3'	5'-CCAGGGCGAGTGTTTGGTCT-3'
DNER	5'-GTGGTGAAGGTCAGCACCTGT-3'	5'-GGCTGAGGGCACAGAAGTCAA-3'
NGFR	5'-GTTCTCCTGCCAGGACAAGCA-3'	5'-GTCCACGGAGATGCCACTGT-3'
LRRN6A	5'-GTACAACCTCAAGTCACTGGAGGT-3'	5'-CATTGAGCACGCGCAGGTAGTT-3'
ECSM2	5'-CAATGACCCAGACCTCTAGCTCT-3'	5'-GCAGCTTTCAGACAGCCCTGA-3'
LGALS3BP	5'-CCCACAGACCTGCTCCAACT-3'	5'-CCGTCTGGACTGATAGACCAGTT-3'
PTPRF	5'-CAGCCCCTACTCGGATGAGAT-3'	5'-GCGATGACATTCGCATAGCGGTT-3'
FCGRT	5'-CTCTCCCTCCTGTACCACCTT-3'	5'-GTGCCCTGCTTGAGGTCGAAAT-3'
LAMP2	5'-GTGCAGTTCGGACCTGGCTT-3'	5'-CAGCTGCCTGTGGAGTGAGTT-3'
RCN1	5'-GACAATGATGGGGATGGCTTTGTCA-3'	5'-CGGAATTCGTTAAACTGCTCCCGTT-3'
MMP14	5'-CAACATTGGAGGAGACACCCACTTT-3'	5'-GTTCCAGGGACGCCTCATCAAA-3'
SDC2	5'-GCTCCATTGAAGAAGCTTCAGGAGT-3'	5'-GCCTTCTGATAAGCAGCACTGGAT-3'
DAG1	5'-CGGAGGCAGATCCATGCTACA-3'	5'-GGCAGTTTCCAATCTGGTGATGGA-3'
EPCR	5'-CTACTTCCGCGACCCCTATCA-3'	5'-GCGAAGTGTAGGAGCGGCTT-3'
CD97	5'-CAAGACAAGCTCAGCCGAGGT-3'	5'-CTCCCCATCGGAGGACTCAA-3'
CD99L2	5'-CAAGAAACCCAGTGCTGGGGAT-3'	5'-GTACGCTGAACAGCTGGCTCT-3'
IGFBP5	5'-CTCAACGAAAAGAGCTACCGCGA-3'	5'-CTGTCGAAGGTGTGGCACTGAA-3'
CLU	5'-CAATGAGACCATGATGGCCCTCT-3'	5'-CCGGGCTATGGAAGTGGATGT-3'
LSAMP	5'-GGACAACATCACCGTGAGGCA-3'	5'-GGAGACCTCGTTGGCAGCTT-3'
NPTN	5'-CCCTGTCACCCTGCAGTGTA-3'	5'-CCAATGGCGTTGGTGGCATTACA-3'
EFNA5	5'-CCAGAGGGGTGACTACCATATTGA-3'	5'-CGGCTGACTCATGTACGGTGT-3'
PODXL	5'-CTCCACAGCCACAGCTAAACCTA-3'	5'-CTGGCAGGGTAGGTGTTCTCAA-3'
TMEM123	5'-CCATGGCGGCATCTGCAAACAT-3'	5'-CGATACCGAATGCCTCTTCTTGAGT-3'
PCOLCE	5'-CGGACGCTTTTGTGGGACCTT-3'	5'-GGCAGCTTGACTTTAGGCTCAGTT-3'
SEZ6L2	5'-GCACCTGCACTTTGAAAGGGTCT-3'	5'-GTCCCCTTCCCGCACATTCAATAT-3'
IGFBP4	5'-GAAGCCCCTGCACACACTGAT-3'	5'-GAAAGCTGTCAGCCAGCTGGT-3'
IGFBP3	5'-GCATCTACACCGAGCGCTGT-3'	5'-GGGACTCAGCACATTGAGGAACTT-3'
LOX	5'-GTCACTGGTTCCAAGCTGGCTA-3'	5'-GGAATATCTTGGTCGGCTGGGTA-3'
CTGF	5'-GCGTGTGCACCGCCAAAGAT-3'	5'-CGGTATGTCTTCATGCTGGTGCA-3'
SPARC	5'-CTGCCAGAACCACCACTGCAA-3'	5'-CTGCCAGTGTACAGGGAAGATGT-3'
QSCN6	5'-GGCTGACCTGGAATCTGCACT-3'	5'-CATTGTGGCAGGCAGAACAAAGTTC-3'
EDIL3	5'-CTGTGAGTGCCCAGGCGAATTTA-3'	5'-GATTTCATACCCAGAGGCTCAGAACA-3'
MXRA8	5'-GTACACCTGCAACCTGCACCAT-3'	5'-GGGACGATGACATTGATGACGTTGT-3'
PRRT3	5'-GCTGACAGTCACAGGAACTCTGA-3'	5'-GCCTCCTGCAAGTGTTCCTCAA-3'
LRP1	5'-CAATGGCCTGACGCTGGACTAT-3'	5'-CGGTGTCACACTTCCACCAGA-3'
ISLR	5'-GCTCGCTGCAACTCAACCACAA-3'	5'-CTCAGCACTGCCCAGCTCATT-3'
COL6A1	5'-GCAGTACAGCCACAGCCAGAT-3'	5'-GTCAAAGTTGTGGCTGCCCAC-3'
TIMP1	5'-GACCTCGTCATCAGGGCCAA-3'	5'-GCAAGGTGACGGGACTGGAA-3'
LAMP1	5'-CACGTTACAGCGTCCAGCTCAT-3'	5'-CCTTGTAGGAAAAACCGGCTAGAAC-3'
SERPINH1	5'-CTGCTGCGCTCACTCAGCAA-3'	5'-CGTGATGGGGCATGAGGATGAT-3'
COL1A1	5'-CACCTCAAGAGAAGGCTCACGAT-3'	5'-CCACGCTGTTCTTGCAGTGGTA-3'
GAPDH	5'-ACCACAGTCCATGCCATCAC-3'	5'-TCCACCACCCTGTTGCTGTA-3'

The RNA sequences used are as follows: siEF1 (sense 5'-GGC AGCAGAACCCUUCUUAdCdG-3', antisense 5'-UAAGA AGGGUUCUGCUGCCdCdG-3'). SJES-5 cells were plated on a 6-well plate and propagated in RPMI-1640 medium supplemented with 10% FBS. Twenty-four hours later, for transfection, 1 μl of 10 pmol siRNA was diluted with 99 μl of Opti-MEM (Invitrogen), and 2 μl of siFECTOR reagent (B-Bridge International, Mountain View, CA, USA) was diluted with 98 μl of Opti-MEM. Both solutions were mixed gently and incubated at room temperature for 5 min. The mixture was diluted with 800 μl of Opti-MEM, and left at room temperature for 15 min. Next, 1 ml of RNA/liposome

Table III. Genes isolated by the retrovirus-mediated signal sequence trap method (SST-REX).

Isolated gene	Accession number[a]	Frequency[b]
Granulin (GRN)	NM_002087	22
Alzheimer disease amyloid ß A4 precursor protein	NM_201414	16
Procollagen-proline, 2-oxoglutarate 4-dioxygenase	NM_000918	14
NODAL modulator 2 (NOMO2)	NM_173614	12
NODAL modulator 1 (NOMO1)	NM_014287	12
NODAL modulator 3 (NOMO3)	NM_001004067	11
Golgi apparatus protein 1 (GLG1)	NM_012201	10
Podocalyxin-like (PODXL)	NM_001018111	6
Lysosomal-associated membrane protein 2 (LAMP2)	NM_013995	6
Insulin-like growth factor binding protein 3 (IGFBP3)	NM_000598	6
Basigin	NM_198589	6
Dystroglycan 1	NM_004393	6
DKFZP56400823 protein	NM_015393	5
Ephrin-A5	NM_001962	4
SPARC	NM_003118	4
CD97	NM_001025160	4
Calreticulin	NM_004343	4
Insulin-like growth factor binding protein 4 (IGFBP4)	NM_001552	4
Poliovirus receptor	NM_006505	3
Syndecan 2	NM_002998	3
Seizure-related 6 homolog like 2	NM_201575	3
CD276	NM_025240	3
TMED7	NM_181836	3
Ribophorin II	NM_002951	3
Niemann-Pick disease, type C1	NM_000271	3
TMEM165	NM_018475	3
MHC class I antigen	NM_005514	3
Colony stimulating factor 2	NM_000758	3
NGFR	NM_002507	2
Ribophorin I	NM_002950	2
Proline-rich transmembrane protein 3	NM_207351	2
Custerin	NM_203339	2
Prosaposin	NM_002778	2
Leucine rich repeat neuronal 6A (LRRN6A)	NM_032808	2
Lysosomal-associated membrane protein 1 (LAMP1)	NM_005561	2
Quiescin Q6	NM_001004128	2
Neuroplastin	NM_017455	2
Reticulocalbin 1	NM_002901	2
Hemicentin 1	NM_031935	2
Matrix metallopeptidase 14 (MMP14)	NM_004995	2
Collagen, type VI, α1	NM_001848	2
MHC class I polypeptide-related sequence A	NM_000247	2
Low density lipoprotein-related protein 1 (LRP1)	NM_002332	2
TMEM123	NM_052932	2
Collagen, type XV, α1	NM_001855	2
Protein kinase C substrate 80K-H	NM_002743	2
EGF-like module containing, mucin-like, hormone receptor-like 2	NM_152920	2
Collagen, type I, α2	NM_000089	2
Lectin, galactoside-binding, soluble, 3 binding protein	NM_005567	2
Collagen, type VII, α1	NM_000094	2

Table III. Continued.

Isolated gene	Accession number[a]	Frequency[b]
Protein tyrosine phosphatase, receptor type, F	NM_130440	1
Connective tissue growth factor	NM_001901	1
Protein disulfide isomerase family A, member 4	NM_004911	1
Immunoglobulin superfamily containing leucine-rich repeat (ISLR)	NM_005545	1
Collagen, type I, α1	NM_000088	1
Procollagen C-endopeptidase enhancer (PCOLCE)	NM_002593	1
Chromosome 1 open reading frame 56	NM_017860	1
TIMP metallopeptidase inhibitor 1 (TIMP1)	NM_003254	1
Insulin-like growth factor binding protein 5 (IGFBP5)	NM_000599	1
Solute carrier family 24 member 6 (SLC24A6)	NM_024959	1
Neural cell adhesion molecule 2 (NCAM2)	NM_004540	1
Collagen, type V, α1	NM_000093	1
CD248	NM_020404	1
Fc fragment of IgG, receptor, transporter, α	NM_004107	1
Nucleobindin 1	NM_006184	1
delta/notch-like EGF-related receptor (DNER)	NM_139072	1
Limbic system-associated membrane protein (LSAMP)	NM_002338	1
Lysyl oxidase (LOX)	NM_002317	1
Endothelial cell-specific molecule 2 (ECSM2)	NM_001077693	1
Isolate Tor36 (ZE657) mitochondrion	AY738975	1
Lectin, mannose-binding, 1	NM_005570	1
CD99 molecule-like 2	NM_031462	1
EGF-like repeats and discoidin I-like domains 3	NM_005711	1
SIL1 homolog, endoplasmic reticulum chaperone	NM_022464	1
ADAM with thrombospondin type 1 motif, 4 (ADAMTS4)	NM_005099	1
Matrix-remodelling associated 8 (MXRA8)	NM_032348	1
Protein C receptor, endothelial	NM_006404	1
Tissue factor pathway inhibitor	NM_001032281	1
Serpin peptidase inhibitor, clade H member 1 (SERPINH1)	NM_001235	1
Protocadherin γ subfamily A.6	NM_032086	1

[a]Accession number in GenBank protein database. [b]Number of the clones isolated by SST-REX.

complex was added to 1 ml of OPTI-MEM supplemented with 20% FBS. Then, the culture medium of the SJES-5 cells was replaced with the 2 ml of the RNA/liposome-containing medium prepared. Twenty-four hours after transfection, culture medium was replaced with the 2 ml of Opti-MEM with 10% FBS, and grown for another 48 h. The cells were harvested and then total RNA was extracted for RT-PCR analysis. The primers used for RT-PCR are as follows: EWS-FLI1-S, 5'-GGGTATGGCACTGGTGCTTATGAT-3'; EWS-FLI1-AS, 5'-GGCTCCAAAGAAGCTGGAGGAA-3'; EWS-S, 5'-GCCCAGCCCACTCAAGGATAT-3'; EWS-AS, 5'-CCC CTGTGCTAGATTGAGGTTGA-3'; FLI1-S, 5'-GCCAACG CCAGCTGTATCA-3'; FLI1-AS, 5'-GTGTGAAGGCACGT GGGTGTT-3'.

IP-Western analysis. IP-Western blot analysis was performed as previously described (39) with some modifications. Briefly, cells were lysed in RIPA buffer [50 mM Tris-HCl (pH 7.4), 150 mM NaCl, 1% NP40, 0.5% deoxycholate, 0.1% SDS]. Cell lysates were immunoprecipitated with the rabbit polyclonal anti-ADAMTS4 antibody. SDS-polyacrylamide gel electrophoresis was performed under reducing conditions using 5-20% gradient gel (Wako Pure Chemical Industries, Osaka, Japan). After transfer to a nitrocellulose membrane, the blot was probed with the rabbit polyclonal anti-ADAMTS4 antibody and then with the HRP-conjugated goat anti-rabbit IgG secondary antibody. ADAMTS4 protein was detected with enhanced chemiluminescence (ECL) Western blotting detection reagents (Santa Cruz Biotechnology).

Immunohistochemical staining. Specimens were retrieved from the patients during surgical resection. Archival tumor blocks were fixed with 10% formaldehyde/phosphate-buffered saline (PBS), and embedded in paraffin. The paraffin-embedded tissues, measuring 4 μm in thickness, were placed on glass slides (Matsunami Glass, Osaka, Japan) and deparaf-

Table IV. Comparison of the gene expression levels between human mesenchymal stem cells (hMSCs) and Ewing's sarcoma (EWS) cells.

A.	hMSC		EWS
DKFZP56400823	–		+
ADAMTS4	–		+
DNER	–		+
NGFR	–		+
LRRN6A	–		+
ECSM2	–		+
LGALS3BP	–		+
PTPRF	–		+
FCGRT	–		+
B.	**hMSC**		**EWS**
LAMP2	+	<	++
RCN1	+	<	+
MMP14	+	<	+
SDC2	+	<	+
DAG1	+	<	+
EPCR	+	<	+
CD97	+	<	+
CD99L2	+	<	+
IGFBP5	+	<	+
CLU	+	<	+
LSAMP	+	<	+
NPTN	+	<	+
EFNA5	+	<	+
PODXL	+	<	+
TMEM123	+	<	+
C.	**hMSC**		**EWS**
PCOLCE	+		+
SEZ6L2	+		+
IGFBP4	+		+
IGFBP3	+		+
LOX	+	>	+
CTGF	+	>	+
SPARC	+	>	+
QSCN6	+	>	+
EDIL3	+		+
MXRA8	+		+
PRRT3	+		+
LRP1	+		+
ISLR	+		+
COL6A1	+	>	+
TIMP1	++	>	+
LAMP1	+		+
SERPINH1	+		+
COL1A1	+		+

++, strongly positive; +, modelately positive; –, negative; > or <, >2-fold difference in the expression level.

finized in xylene for hematoxylin and eosin (H&E) and immunohistochemical staining. Antigen retrieval was performed with citrate buffer (pH 6.0) at 97°C for 45 min. After cooling for 60 min and washing in PBS, the rabbit anti-ADAMTS4 antibody (Santa Cruz Biotechnology) diluted 1:50 in antibody diluent buffer (Dako) was reacted. The slides were then washed and incubated with the HRP-conjugated anti-rabbit IgG antibody. The 3-3' diaminobenzidine tetrahydrochloride (DAB) was used for coloration. Hematoxylin was used as the final nuclear counterstaining.

Immunofluorescence staining. The expression of ADAMTS4 protein was analyzed by immunofluorescence. Cells were fixed for 30 min in 4% paraformaldehyde/PBS, and permeabilized for 30 min in 0.1% Triton X/PBS. Fixed cells were rehydrated with Tris-buffered saline, and then incubated with the rabbit polyclonal anti-ADAMTS4 antibody. Immunofluorescence staining was done with the Alexa488-conjugated anti-rabbit IgG antibody. Nucleus was detected with bisbenzimide (Hoechst-33342, Sigma-Aldrich) staining.

ELISA. To evaluate the expression level of secreted ADAMTS4 protein, supernatants of the EWS cell lines and the patient sera were subjected to ELISA. The 96-well plates were coated with the monoclonal anti-human ADAMTS4 antibody at 4°C overnight. After 3 washes with washing buffer (0.05% Tween-20/PBS), the plates were treated with 10% FBS in PBS for 1 h at room temperature. The recombinant human ADAMTS4 (amino acids 213-685) diluted with 10% FBS in PBS, as standard proteins, and the samples were added to each well, and incubated at room temperature for 2 h. After 5 washes with washing buffer, the Avidin-HRP and the biotinylated anti-human ADAMTS4 detection antibody were added to each well, and incubated for 1 h at room temperature. After 7 washes with washing buffer, 100 μl of tetramethylbenzidine buffer as a substrate was added to each well and incubated for 30 min at room temperature in the dark. Color development was stopped by addition of 100 μl of stop solution (1 N H_3PO_4). Optic density of each sample was measured at 450 nm.

Results

Analysis of isolated cDNA clones. In SST-REX screening, we isolated 322 factor-independent Ba/F3 clones (Table III). Sequencing analyses revealed that integrations derived from 256 clones harbored the signal sequence. Among them, 80 different secreted and type I membrane proteins were identified. We used the database of RefEX, PubMed, ONCOMINE and SMART for the analysis, and 42 proteins that might be related to tumor/cancer onset and progression were selected.

Recent studies have suggested that the origin of EWS is derived from hMSC (40,41). To examine the expression levels of these 42 molecules in EWS in comparison with hMSC, we performed RT-PCR analysis (Table IV). They were classified into 3 groups by mRNA expression profiles; the first group with high expression levels only in EWS (Table IVA), the second group with higher expression levels in EWS than in hMSC (Table IVB), and the third group with similar or lower expression levels in EWS compared with

Table V. Gene expression levels in murine tissues by RT-PCR analysis.

	Brain	Heart	Lung	Liver	Kidney	Spl	Stm	S. int	L. int	Mus	Tes	Thy	BM	OC
DKFZP56400823	+	+	+	–	+	+	+	+	+	+	+	+	+	+
ADAMTS4	++	+	–	+	–	–	–	–	–	+	–	–	+	+
DNER	++	–	–	–	–	–	–	–	–	–	+	–	–	+
NGFR	+	+	–	+	+	–	–	–	–	–	–	–	–	–
LRRN6A	++	–	–	–	–	+	–	+	+	+	+	+	+	+
ECSM2	+	+	+	+	+	–	+	–	–	+	+	+	+	+
LGALS3BP	+	+	+	+	+	+	++	++	+	+	++	++	+	+
PTPRF	+	+	+	+	+	–	+	+	+	+	+	+	–	–
FCGRT	+	+	+	+	+	+	+	+	+	+	+	+	+	+
LAMP2	+	++	+	+	++	++	+	+	+	+	+	+	+	+
RCN1	+	+	+	+	+	–	+	–	–	–	+	+	+	+
MMP14	+	+	+	+	+	–	+	–	–	+	+	+	+	+
SDC2	+	+	+	+	+	–	+	+	–	+	+	+	+	+
DAG1	+	+	+	+	+	+	+	+	+	+	+	+	+	+
EPCR	+	+	+	+	+	+	+	–	–	+	+	+	+	++
CD97	+	+	+	+	+	+	+	+	+	+	+	+	+	+
CD99L2	+	+	+	+	+	–	–	–	–	+	+	+	+	+
IGFBP5	+	+	+	+	+	+	+	+	+	+	+	+	+	+
CLU	+	+	+	+	+	+	+	+	–	+	+	+	+	+
LSAMP	++	+	–	+	+	–	+	–	–	–	+	+	+	+
NPTN	+	+	+	+	+	–	+	+	+	+	+	+	+	+
EFNA5	+	+	+	+	+	–	+	+	+	–	+	+	–	–
PODXL	+	+	+	+	+	–	–	–	–	+	–	–	+	–
TMEM123	–	+	–	+	+	–	–	–	–	+	–	–	–	–

Spl, spleen; stm, stomach; s. int, small intestine; l. int, large intestine; mus, muscle; tes, testis; thy, thymus; BM, bone marrow; OC, osteoclast; ++, strongly positive; +, modelately positive; –, negative.

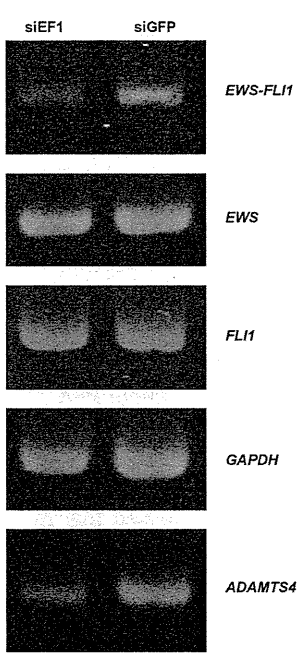

Figure 1. Effects of *EWS-FLI1* suppression on *ADAMTS4* expression. RNA from Ewing's sarcoma cells treated with either siEF1 or siGFP were subjected to RT-PCR experiment. *ADAMTS4* mRNA expression was down-regulated after treatment with *EWS-FLI1*-specific siRNA. *GAPDH* (*glyceraldehyde 3-phosphate dehydrogenase*) was used as an internal control.

hMSC (Table IVC). We picked up 24 molecules from the first and second groups, and examined the expression patterns in murine organs. As shown in Table V, most molecules did not exhibit interesting tissue distribution patterns. However, some of the molecules attracted us by their expression profiles or their novelty as a gene. We focused on 5 molecules: *ADAMTS4*, *DNER* (*delta/notch-like EGF-related receptor*), *NGFR* (*nerve growth factor receptor*), *LRRN6A* (*leucine rich repeat neuronal 6A*) and *ECSM2* (*endothelial cell-specific molecule 2*). We then examined expression levels of these 5 molecules in various solid tumor and hematopoietic cell lines by RT-PCR. As shown in Table VI, expression levels of *ADAMTS4* were higher in EWS, glioblastoma and neuroblastoma in comparison with other cell lines. These results suggested that *ADAMTS4* is one of the first candidate molecules as a marker for EWS among the SST clones.

ADAMTS4 expression is upregulated by EWS-FLI1. Previous studies indicated the expression of the fusion gene, *EWS-FLI1*, was suppressed by using antisense oligonucleotide or siRNA. To decrease the expression level of *EWS-FLI1* in the EWS cell line, we made an siRNA duplex specifically directed against the fusion junction of *EWS-FLI1* transcript. *EWS-FLI1*-specific siRNA (siEF1) was used for SJES-5 cell line. As a control, siGFP was also used. Transfection of siEF1,

Table VI. Gene expression levels of *ADAMTS4*, *DNER*, *NGFR*, *LRRN6A* and *ECSM2* in human cancer cell lines by RT-PCR analysis.

	ADAMTS4	DNER	NGFR	LRRN6A	ECSM2
AsPC-1	–	–	+	–	–
BxPC-3	–	+	–	–	–
Capan-1	–	–	–	–	–
U87MG	+	+	–	–	–
U251	+	++	–	–	–
T98G	–	+	–	–	–
HGC-27	+	–	+	+	–
MKN45	–	+	–	++	–
GCIY	+	+	–	+	–
KATOIII	–	–	–	–	–
MG63	–	+	+	+	+
HOS	+	+	+	+	+
KHOS/NP	–	+	+	+	+
SaOS2	–	+	+	–	–
U2OS	–	+	+	+	–
KPNSI-FA	+	++	+	+	–
LAN-1	+	+	+	+	–
NB69	++	–	+	+	+
H460	+	++	–	+	–
PLC/PRF/5	–	+	+	+	+
HuCCT1	–	++	–	+	+
SW48	–	+	+	–	+
RMS	++	++	+	++	+
SJRH-30	++	+	+	+	+
SJES-2, 3, 5, 6, 7, 8	++	++	+	++	++
MOLM13	–	–	–	–	–
ML1	–	–	–	–	–
U937	–	–	–	–	+
Jurkat	–	–	–	–	+
PEER	–	–	–	–	+
CEM	++	–	–	–	+
HPB-ALL	–	–	–	–	–
NALM24	+	+	–	–	+
NALM16	–	+	+	–	–
IM9	–	–	+	–	+

++, strongly positive; +, moderately positive; –, negative.

but not siGFP, led to significant decrease of the expression level of the *EWS-FLI1* fusion transcript (Fig. 1). In agreement with the specificity of siEF1 against the *EWS-FLI1* fusion gene, the expression level of *EWS* or *FLI1* was not affected. Interestingly, suppression of *EWS-FLI1* expression resulted in decreased expression of *ADAMTS4* transcript. These results suggested that *ADAMTS4* expression was upregulated by EWS-FLI1.

Immunohistochemical analysis on ADAMTS4 protein expression. In order to confirm the expression of ADAMTS4 in EWS at the protein level, we stained 25 tissue samples derived from EWS patients with the anti-ADAMTS4 antibody together with the H&E staining. ADAMTS4 protein was detected in 10 EWS samples, but not in 15 samples where tumors disappeared by chemotherapy (Fig. 2 and data not shown).

Next, to examine the subcellular localization of ADAMTS4, we stained EWS cell lines with the anti-ADAMTS4 antibody. Immunofluorescence microscopy revealed that ADAMTS4 protein was expressed mainly in the cytoplasm of EWS cell lines (Fig. 3C and D) and of the

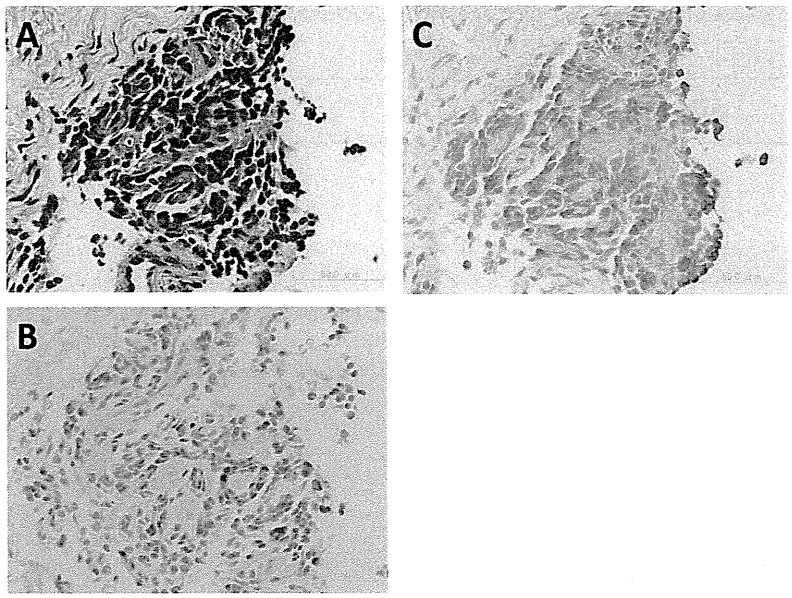

Figure 2. Immunohistochemical analysis of ADAMTS4 protein in the tissue section of the patient with Ewing's sarcoma. (A) Hematoxylin and eosin staining, (B) rabbit IgG, (C) anti-ADAMTS4 antibody.

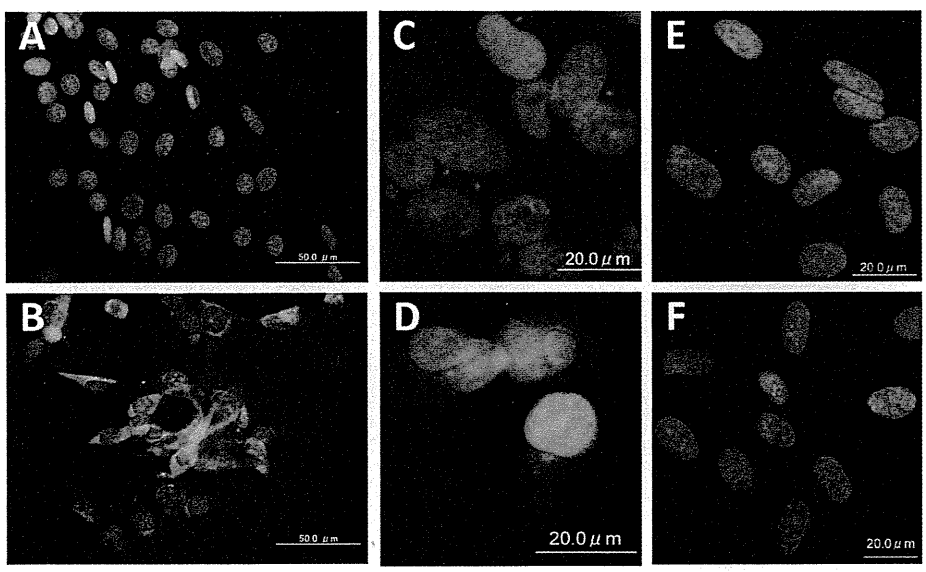

Figure 3. Immunofluorescence staining of ADAMTS4 protein in Ewing's sarcoma cell lines (SJES-2 and SJES-5), osteosarcoma cell lines (MG63 and SaOS2) and NIH3T3 cells expressing ADAMTS4. (A) NIH3T3, (B) ADAMTS4/NIH3T3, (C) SJES-5, (D) SJES-2, (E) MG63, (F) SaOS2.

NIH3T3 cells expressing human ADAMTS4 (Fig. 3B). In contrast, ADAMTS4 was not detected in osteosarcoma cell lines MG63 and SaOS2 (Fig. 3E and F), which did not express *ADAMTS4* at the transcription level (Table VI).

ADAMTS4 is secreted from EWS cells. We next asked whether ADAMTS4 was secreted from EWS cells. First the immunoprecipitates of the cell lysates of EWS cell lines and positive and negative control cells with the anti-ADAMTS4 antibody were electrophoresed, blotted and probed with the same antibody. ADAMTS4 was detcted in EWS cells and the positive control cells as double bands of ~100 kDa (Fig. 4A). We next performed the same experiments using 2 ml each of the supernatants of these cells. Notably, significant levels of expression of ADAMTS4 protein were observed in the supernatants of EWS cells and ADAMTS4/NIH3T3 cells (Fig. 4B). These results suggested that ADAMTS4 was secreted.

Comparative study of ADAMTS4 gene expression in 5 types of sarcomas. We showed that *ADAMTS4* transcripts were expressed in EWS, osteosarcoma and rhabdomyosarcoma cell lines (Table VI). However, whether *ADAMTS4* transcripts are expressed in tumor tissue samples remained unknown. Therefore, we tested if *ADAMTS4* was expressed in soft tissue sarcomas and bone tumors including osteosarcoma, EWS, chondrosarcoma, synovial sarcoma and rhabdomyosarcoma (Fig. 5). Benign tumors including lipoma, desmoid

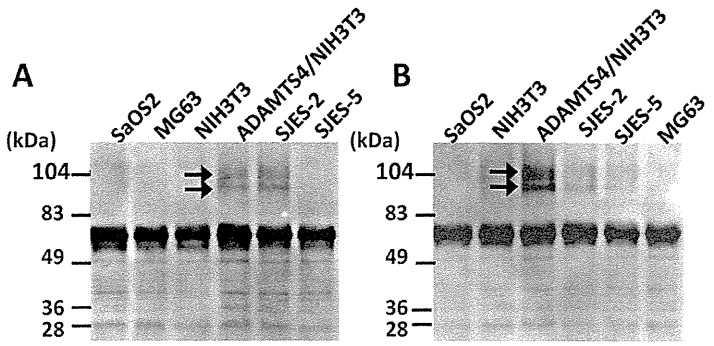

Figure 4. Detection of secreted ADAMTS4 protein. The cell lysates or culture supernatants were immunoprecipitated with the anti-ADAMTS4 antibody, resolved by SDS-PAGE, blotted and probed with the anti-ADAMTS4 antibody. Molecular size markers are shown on the left. Arrows indicate the ADAMTS4 proteins. (A), cell lysates; (B), supernatants.

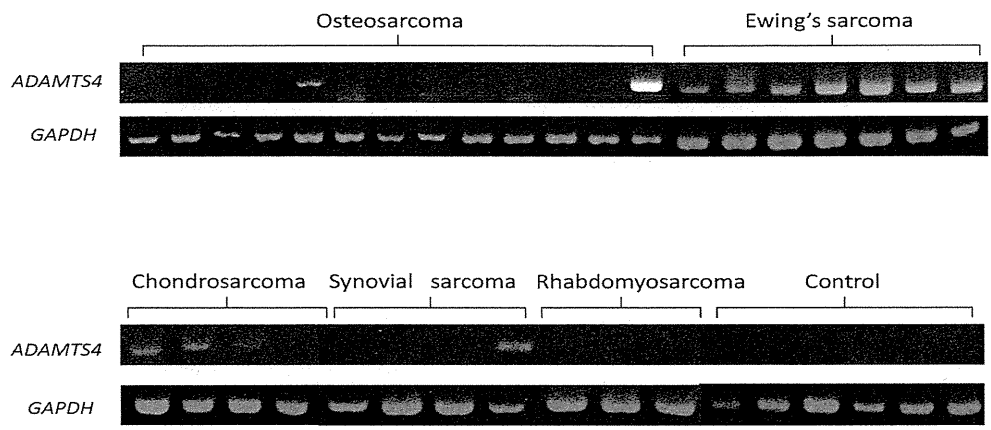

Figure 5. RT-PDR analysis of *ADAMTS4* expression in the patient samples. *GAPDH* expression was used as an internal control.

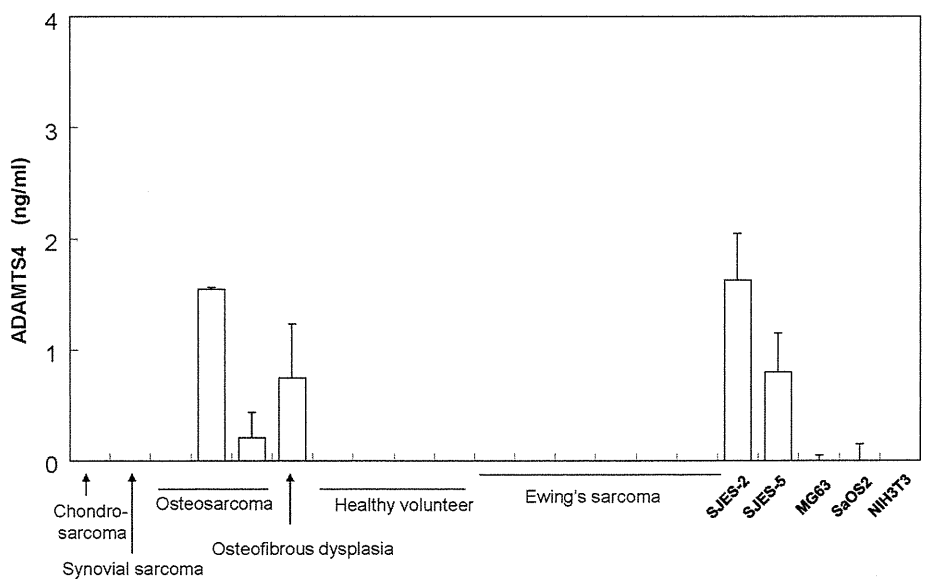

Figure 6. ELISA of ADAMTS4 protein in the patient sera and the supernatants of the cell lines. The error bars represent 1 standard deviation.

and Schwannoma were also examined as controls. In all 7 EWS samples, *ADAMTS4* transcripts were highly expressed. Three out of 4 samples of chondrosarcoma moderately expressed *ADAMTS4*. This result was predictable, since *ADAMTS4* is expressed in normal cartilage cells. Also, 2 out of 13 samples of osteosarcoma and 1 out of 4 samples of synovial sarcoma expressed *ADAMTS4*. *ADAMTS4* transcripts were not detected in the 3 samples of rhabdomyo-

sarcoma, while those were highly expressed in rhabdomyosarcoma cell lines RMS and SJRH-30 (Table VI). Benign tumors examined did not express *ADAMTS4*.

No detection of secreted ADAMTS4 protein in the patient sera. To evaluate the amount of secreted ADAMTS4 protein in the patients, we analyzed ADAMTS4 protein levels in sera by ELISA. In agreement with the results described above, ADAMTS4 was detected in culture supernantants of EWS cell lines SJES-2 and SJES-5 (Fig. 6). The concentration of ADAMTS4 in SJES-2 cells was about twice as high as that in SJES-5 cells. For a positive control, culture supernatant of the NIH3T3/ADAMTS4 cells was also measured (39.9 ng/ml, data not shown). It is noteworthy that ADAMTS4 protein was detected in 2 out of 3 cases of osteosarcoma and in the only case of osteofibrous dysplasia. Consistent with the very high level of *ADAMTS4* transcript shown in the extreme right lane among osteosarcoma samples in Fig. 5, serum from the same patient showed the high level of ADAMTS4 protein in ELISA as shown in Fig. 6 (middle lane among osteosarcoma samples). The other positive samples of osteosarcoma in both figures are not derived from the same patient, because only either serum or RNA was available in these two patients. ADAMTS4 protein was not detected in the 6 EWS patient sera examined. These results indicated that ADAMTS4 is expressed and secreted in EWS cells, but that the ADAMTS4 protein in the serum is not suitable as a marker for EWS.

Discussion

EWS is an aggressive neoplasm with a strong propensity to spread into neighboring tissues. Many patients are diagnosed at advanced stages of EWS. Since EWS has worse prognosis than other soft-tissue sarcomas, it is clinically important to distinguish EWS from other sarcomas. The reason for the poor prognosis in EWS patients is suggested to be that the micro-metastases are formed before clinical symptoms arise and tumors are detected (42). Currently, diagnosis of EWS is determined mainly by CD99 expression or by genetic aberrations that are exemplified by *EWS-FLI1* fusion gene. Since both markers show lack of sensitivity, specificity or feasibility, more useful biomarkers such as surface antigens or secreted proteins are required in clinical areas.

In the present study, we searched for membrane and secreted proteins derived from EWS cell lines using the retrovirus-mediated signal sequence trap method SST-REX, and identified ADAMTS4 as a possible EWS marker. We demonstrated that ADAMTS4 was expressed in EWS cell lines and tissue samples derived from EWS patients. Interestingly, expression of *ADAMTS4* was correlated with expression of *EWS-FLI1*, which is a hallmark of EWS. In addition, we demonstrated that ADAMTS4 was secreted from EWS cells, although we could not detect ADAMTS4 in serum samples derived from EWS patients.

It should be noted that two cases of the osteosarcoma patient samples were found to express high levels of *ADAMTS4*. It is tempting to speculate that a subclass of osteosarcoma with different property may exist.

In conclusion, we identified *ADAMTS4* as a possible marker of EWS by using SST-REX. This is the first report to show the correlation between *ADAMTS4* and EWS. Although ADAMTS4 protein in the serum could not be used as a biomarker for EWS, our study suggested that RNA transcripts of *ADAMTS4* in the tissue sections are useful markers of EWS. Further studies will be required to determine the usefulness of this molecule in differential diagnosis and/or evaluation of the disease activity in clinical settings.

Acknowledgements

We gratefully thank Ms. S. Shoma (The University of Tokyo) for technical support and Dr Y. Murakami (The University of Tokyo) and Dr Y. Fukuchi (Keio University) for helpful comments on this study. This work was supported by a Grant-in-Aid for Cancer Research from the Ministry of Health, Labour and Welfare of Japan.

References

1. Jaffe R, Santamaria M, Yunis EJ, Tannery NH, Agostini RM, Medina J Jr and Goodman M: The neuroectodermal tumor of bone. Am J Surg Pathol 8: 885-898, 1984.
2. Hashimoto H, Enjoji M, Nakajima T, Kiryu H and Daimaru Y: Malignant neuroepithelioma (peripheral neuroblastoma). A clinicopathologic study of 15 cases. Am J Surg Pathol 7: 309-318, 1983.
3. Khoury JD: Ewing sarcoma family of tumors. Adv Anat Pathol 12: 212-220, 2005.
4. Turc-Carel C, Philip I, Berger MP, Philip T and Lenoir G: Chromosomal translocation (11; 22) in cell lines of Ewing's sarcoma. C R Seances Acad Sci III 296: 1101-1103, 1983.
5. Zucman J, Delattre O, Desmaze C, *et al*: Cloning and characterization of the Ewing's sarcoma and peripheral neuroepithelioma t(11;22) translocation breakpoints. Genes Chromosomes Cancer 5: 271-277, 1992.
6. Sorensen PH, Lessnick SL, Lopez-Terrada D, Liu XF, Triche TJ and Denny CT: A second Ewing's sarcoma translocation, t(21;22), fuses the EWS gene to another ETS-family transcription factor, ERG. Nat Genet 6: 146-151, 1994.
7. Jeon IS, Davis JN, Braun BS, Sublett JE, Roussel MF, Denny CT and Shapiro DN: A variant Ewing's sarcoma translocation (7;22) fuses the EWS gene to the ETS gene ETV1. Oncogene 10: 1229-1234, 1995.
8. Arvand A and Denny CT: Biology of EWS/ETS fusions in Ewing's family tumors. Oncogene 20: 5747-5754, 2001.
9. May WA, Gishizky ML, Lessnick SL, Lunsford LB, Lewis BC, Delattre O, Zucman J, Thomas G and Denny CT: Ewing sarcoma 11;22 translocation produces a chimeric transcription factor that requires the DNA-binding domain encoded by FLI1 for transformation. Proc Natl Acad Sci USA 90: 5752-5756, 1993.
10. Ohno T, Rao VN and Reddy ES: EWS/Fli-1 chimeric protein is a transcriptional activator. Cancer Res 53: 5859-5863, 1993.
11. Jambhekar NA, Bagwan IN, Ghule P, Shet TM, Chinoy RF, Agarwal S, Joshi R and Amare Kadam PS: Comparative analysis of routine histology, immunohistochemistry, reverse transcriptase polymerase chain reaction, and fluorescence in situ hybridization in diagnosis of Ewing family of tumors. Arch Pathol Lab Med 130: 1813-1818, 2006.
12. Llombart-Bosch A and Navarro S: Immunohistochemical detection of EWS and FLI-1 proteinss in Ewing sarcoma and primitive neuroectodermal tumors: comparative analysis with CD99 (MIC-2) expression. Appl Immunohistochem Mol Morphol 9: 255-260, 2006.
13. Bernstein M, Kovar H, Paulussen M, Randall RL, Schuck A, Teot LA and Juergens H: Ewing's sarcoma family of tumors: current management. Oncologist 11: 503-519, 2006.
14. Folpe AL, Hill CE, Parham DM, O'Shea PA and Weiss SW: Immunohistochemical detection of FLI-1 protein expression: a study of 132 round cell tumors with emphasis on CD99-positive mimics of Ewing's sarcoma/primitive neuroectodermal tumor. Am J Surg Pathol 24: 1657-1662, 2000.
15. Bernard G, Zoccola D, Deckert M, Breittmayer JP, Aussel C and Bernard A: The E2 molecule (CD99) specifically triggers homotypic aggregation of $CD4^+$ $CD8^+$ thymocytes. J Immunol 154: 26-32, 1995.

16. Zhang PJ, Barcos M, Stewart CC, Block AW, Sait S and Brooks JJ: Immunoreactivity of MIC2 (CD99) in acute myelogenous leukemia and related diseases. Mod Pathol 13: 452-458, 2000.
17. Tashiro K, Tada H, Heilker R, Shirozu M, Nakano T and Honjo T: Signal sequence trap: a cloning strategy for secreted proteins and type I membrane proteins. Science 261: 600-603, 1993.
18. Shirozu M, Nakano T, Inazawa J, Tashiro K, Tada H, Shinohara T and Honjo T: Structure and chromosomal localization of the human stromal cell-derived factor 1 (SDF1) gene. Genomics 28: 495-500, 1995.
19. Kojima T, Morikawa Y, Copeland NG, Gilbert DJ, Jenkins NA, Senba E and Kitamura T: TROY, a newly identified member of the tumor necrosis factor receptor superfamily, exhibits a homology with Edar and is expressed in embryonic skin and hair follicles. J Biol Chem 275: 20742-20747, 2000.
20. Ohta K, Lupo G, Kuriyama S, Keynes R, Holt CE, Harris WA, Tanaka H and Ohnuma S: Tsukushi functions as an organizer inducer by inhibition of BMP activity in cooperation with chordin. Dev Cell 7: 347-358, 2004.
21. Ikeda Y, Imai Y, Kumagai H, Nosaka T, Morikawa Y, Hisaoka T, Manabe I, Maemura K, Nakaoka T, Imamura T, Miyazono K, Komuro I, Nagai R and Kitamura T: Vasorin, a transforming growth factor beta-binding protein expressed in vascular smooth muscle cells, modulates the arterial response to injury in vivo. Proc Natl Acad Sci USA 101: 10732-10737, 2004.
22. Izawa K, Kitaura J, Yamanishi Y, Matsuoka T, Oki T, Shibata F, Kumagai H, Nakajima H, Maeda-Yamamoto M, Hauchins JP, Tybulewicz VL, Takai T and Kitamura T: Functional analysis of activating receptor LMIR4 as a counterpart of inhibitory receptor LMIR3. J Biol Chem 282: 17997-18008, 2007.
23. Ganju RK, Brubaker SA, Meyer J, Dutt P, Yang Y, Qin S, Newman W and Groopman JE: The alpha-chemokine, stromal cell-derived factor-1alpha, binds to the transmembrane G-protein-coupled CXCR-4 receptor and activates multiple signal transduction pathways. J Biol Chem 273: 23169-23175, 1998.
24. Kitamura T, Onishi M, Kinoshita S, Shibuya A, Miyajima A and Nolan GP: Efficient screening of retroviral cDNA expression libraries. Proc Natl Acad Sci USA 92: 9146-9150, 1995.
25. Kojima T and Kitamura T: A signal sequence trap based on a constitutively active cytokine receptor. Nat Biotechnol 17: 487-490, 1999.
26. Kuno K, Kanada N, Nakashima E, Fujiki F, Ichimura F and Matsushima K: Molecular cloning of a gene encoding a new type of metalloproteinase-disintegrin family protein with thrombospondin motifs as an inflammation associated gene. J Biol Chem 272: 556-562, 1997.
27. Porter S, Clark IM, Kevorkian L and Edwards DR: The ADAMTS metalloproteinases. Biochem J 386: 15-27, 2005.
28. Tortorella MD, Burn TC, Pratta MA, *et al*: Purification and cloning of aggrecanase-1: a member of the ADAMTS family of proteins. Science 284: 1664-1666, 1999.
29. Tortorella MD, Malfait AM, Deccico C and Arner E: The role of ADAM-TS4 (aggrecanase-1) and ADAM-TS5 (aggrecanase-2) in a model of cartilage degradation. Osteoarthritis Cartilage 9: 539-552, 2001.
30. Sandy JD, Neame PJ, Boynton RE and Flannery CR: Catabolism of aggrecan in cartilage explants. Identification of a major cleavage site within the interglobular domain. J Biol Chem 266: 8683-8685, 1991.
31. Sandy JD, Flannery CR, Neame PJ and Lohmander LS: The structure of aggrecan fragments in human synovial fluid. Evidence for the involvement in osteoarthritis of a novel proteinase which cleaves the Glu 373-Ala 374 bond of the interglobular domain. J Clin Invest 89: 1512-1516, 1992.
32. Lohmander LS, Neame PJ and Sandy JD: The structure of aggrecan fragments in human synovial fluid. Evidence that aggrecanase mediates cartilage degradation in inflammatory joint disease, joint injury, and osteoarthritis. Arthritis Rheum 36: 1214-1222, 1993.
33. Kashiwagi M, Tortorella M, Nagase H and Brew K: TIMP-3 is a potent inhibitor of aggrecanase 1 (ADAM-TS4) and aggrecanase 2 (ADAM-TS5). J Biol Chem 276: 12501-12504, 2001.
34. Yamanishi Y, Boyle DL, Clark M, Maki RA, Tortorella MD, Arner EC and Firestein GS: Expression and regulation of aggrecanase in arthritis: the role of TGF-beta. J Immunol 168: 1405-1412, 2002.
35. Matthews RT, Gary SC, Zerillo C, Pratta M, Solomon K, Arner EC and Hockfield S: Brain-enriched hyaluronan binding (BEHAB)/brevican cleavage in a glioma cell line is mediated by a disintegrin and metalloproteinase with thrombospondin motifs (ADAMTS) family member. J Biol Chem 275: 22695-22703, 2000.
36. Morita S, Kojima T and Kitamura T: Plat-E: an efficient and stable system for transient packaging of retroviruses. Gene Ther 7: 1063-1066, 2000.
37. Kitamura T, Koshino Y, Shibata F, Oki, T, Nakajima H, Nosaka T and Kumagai H: Retrovirus-mediated gene transfer and expression cloning: powerful tools in functional genomics. Exp Hematol 11: 1007-1014, 2003.
38. Prieur A, Tirode F, Cohen P and Delattre O: EWS/FLI-1 silencing and gene profiling of Ewing cells reveal downstream oncogenic pathways and a crucial role for repression of insulin-like growth factor binding protein 3. Mol Cell Biol 24: 7275-7283, 2004.
39. Nosaka T, Kawashima T, Misawa K, Ikuta K, Mui AL and Kitamura T: STAT5 as a molecular regulator of proliferation, differentiation and apoptosis in hematopoietic cells. EMBO J 18: 4754-4765, 1999.
40. Tirode F, Laud-Duval K, Prieur A, Delorme B, Charbord P and Delattre O: Mesenchymal stem cell features of Ewing tumors. Cancer Cell 11: 421-429, 2007.
41. Riggi N, Cironi L, Provero P, Suva ML, Kaloulis K, Garcia-Echeverria C, Hoffmann F, Trumpp A and Stamenkovic I: Development of Ewing's sarcoma from primary bone marrow-derived mesenchymal progenitor cells. Cancer Res 65: 11459-11468, 2005.
42. Schleiermacher G, Peter M, Oberlin O, Philip T, Rubie H, Mechinaud F, Sommelet-Olive D, Landman-Parker J, Bours D, Michon J and Delattre O: Increased risk of systemic relapses associated with bone marrow micrometastasis and circulating tumor cells in localized Ewing tumor. J Clin Oncol 21: 85-91, 2003.

Podoplanin Expression in Cancerous Stroma Induces Lymphangiogenesis and Predicts Lymphatic Spread and Patient Survival

Haruhisa Kitano, MD; Shun-Ichiro Kageyama, PhD; Stephen M. Hewitt, MD, PhD; Ryuji Hayashi, MD, PhD; Yoshinori Doki, MD, PhD; Yoshitomo Ozaki, MD, PhD; Shozo Fujino, MD, PhD; Mikiko Takikita, MD, PhD; Hajime Kubo, MD, PhD; Junya Fukuoka, MD, PhD

• ***Context.***—**Podoplanin is a mucin-type glycoprotein and a lymphatic endothelial marker. Immunohistochemical staining for podoplanin is currently used as a routine pathologic diagnosis tool in Japan to identify lymphatic invasion of cancer cells. Recent reports suggest that podoplanin and other proangiogenic molecules are expressed in stromal fibroblasts and myofibroblasts.**

Objective.—**To analyze the distribution of podoplanin expression in tumor stroma and its clinical and biologic significance.**

Design.—**We performed immunohistochemistry for podoplanin on tissue microarrays from 1350 cases of 14 common cancer types.**

Results.—**Two hundred eighty-seven of 662 cases (43%) showed podoplanin expression in the stromal cells within cancer nests. Stromal podoplanin expression in 14 common cancer types was significantly associated with tumor stage ($P < .001$), lymph node metastases ($P < .001$), lymphatic invasion ($P = .02$), and venous invasion ($P < .001$). The stromal cells positive for podoplanin were also positive for α-smooth muscle actin but negative for desmin, confirming a myofibroblasts phenotype. In contrast, myofibroblasts in inflammatory fibrotic lung diseases were podoplanin negative. Lymphatic vessel density was greater in the stromas with podoplanin expression than in the stroma lacking podoplanin-expressing stromal cells ($P = .01$). Survival data were available for non–small cell lung cancer. Stromal podoplanin expression was associated with poorer prognosis in adenocarcinoma ($P < .001$) and remains statistically significant after adjustment for sex, age, and stage ($P = .01$).**

Conclusion.—**Our data indicate that podoplanin expression in stromal myofibroblasts may function as a proangiogenic biomarker and may serve as a predictive marker of lymphatic/vascular spread of cancer cells and a prognostic marker of patient survival.**

(*Arch Pathol Lab Med.* 2010;134:1520–1527)

The recent identification of lymphatic endothelial markers has enabled the specific identification of lymphatic vessels.[1–3] Among them, the mucin-type transmembrane glycoprotein podoplanin (also known as T1, gp38, D2-40, or Aggrus) is a well-established marker specific for lymphatic-endothelial cells and is not expressed in blood vessel endothelial cells.[3]

Identification of lymphatic, as well as vascular, invasion by cancer cells is often a negative prognostic factor[4,5] and is used in routine diagnostic pathology in Japan. Podoplanin is often used to detect lymphatic involvement by cancer cells in various cancer types. For colon cancer, use of podoplanin to identify lymphatic involvement is recommended by some Japanese cancer treatment guidelines.[6] With increasing routine use of immunohistochemistry for podoplanin, we have observed frequent podoplanin expression in cancerous stromal cells, most commonly in association with colon cancer. Apart from lymphatic endothelial cells, expression of podoplanin in tumor cells has been reported in some cancer types including squamous cell carcinoma in the lung,[7–10] malignant mesothelioma,[11,12] Kaposi sarcoma, angiosarcoma,[13] hemangioblastoma,[14] dysgerminoma,[7] and brain tumors.[15–17] Recent reports suggest that podoplanin expression in cancer cells may be associated with tumor invasion, metastases, or poor prognosis, although the detailed mechanisms remain obscure.[3,10,17]

Previous publications have reported that podoplanin expression may contribute to lymphatic metastasis in intrahepatic cholangiocarcinoma and have called attention to their presence in cancer-associated fibroblasts of lung adenocarcinoma.[18,19] In our study, we focused on podoplanin expression in stromal cells and investigated

Accepted for publication January 18, 2010.

From the Laboratory of Pathology, Toyama University Hospital, Toyama, Japan (Drs Kitano, Kageyama, and Fukuoka); the Department of Surgery, Shiga University of Medical Science, Otsu, Japan (Drs Kitano, Ozaki, and Fujino); Tissue Array Research Program, Laboratory of Pathology, Center for Cancer Research, National Cancer Institute, National Institutes of Health, Bethesda, Maryland (Drs Hewitt and Takikita); the Departments of Internal Medicine (Dr Hayashi) and Surgery (Dr Doki), Toyama University, Toyama, Japan; and the Division of Gastrointestinal Surgery, Department of Surgery, Kyoto University Hospital, Kyoto, Japan (Dr Kubo).

The authors have no relevant financial interest in the products or companies described in this article.

Reprints: Junya Fukuoka, MD, PhD, Department of Surgical Pathology, Toyama Tissue Microarray Laboratory, Toyama University Hospital, 2630 Sugitani, Toyama, 930-0194, Japan (e-mail: fukuokaj@med.u-toyama.ac.jp).

its clinicopathologic characteristics among common cancer types and its association with prognosis in lung cancer.

MATERIALS AND METHODS

Clinical Samples

A total of 1350 cancer cases (400 lung cancer cases; 100 cases each of breast, kidney, biliary tract, thyroid, liver, colon, and stomach cancer; and 50 cases each of prostate, pancreas, bladder, ovary, and uterine body cancer) were selected from the pathology case archive of Toyama University Hospital based on the diagnosis and the quality of the available tissue on the paraffin block. This study was approved by the ethics committee at Toyama University. A total of 1152 patients had adequate clinical and pathologic information. These patients did not receive neoadjuvant treatment. Survival time data and outcome were limited to 211 of 400 lung cancers. The tumors were pathologically staged according to the International Union Against Cancer's TNM classification and histologically divided and graded according to the 2004 World Health Organization guidelines.[20]

Composition of Tissue Microarrays

Two high-density tissue microarrays (TMAs) were designed. The first TMA has 1150 cores from 14 common cancer types (multiple cancer TMA). The second contains 1200 cores representing 400 lung cancer cases in duplicate along with nonneoplastic lung tissue cores from the same patients (lung cancer TMA). For each case, the area with the most representative histology was selected from review of hematoxylin-eosin–stained slides. The cylindrical tissue samples (0.6 mm) were cored from the previously described areas in the donor blocks and extruded into the recipient array blocks using a manual tissue microarrayer (Beecher Instruments, Silver Spring, Maryland) as previously described.[20,21] Multiple 4-μm sections were cut with a microtome using an adhesive-coated tape (Instrumedics, St Louis, Missouri) and stored until use as previously described.[20] Hematoxylin-eosin staining of TMA slides was examined every 50th section to confirm the presence of tumor cells.

Immunohistochemical Staining for TMAs

For all antibodies, the same protocol was used. After sections were deparaffinized and hydrated, antigen retrieval was performed using a pressure chamber (Pascal, DAKO, Kyoto, Japan) in which tissues were heated to 125°C, kept for 1 minute, and cooled to 90°C. After rinsing, slides were placed in an Autostainer (DAKO) and an Envision+ detection system was applied as suggested by the manufacturer's protocol (DAKO). The anti-human podoplanin monoclonal antibody was generated in Kyoto University.[22] The specificity and sensitivity of the antibody, clone 7B10, was examined and reported using enzyme-linked immunosorbent assay, Western blot analyses, and immunohistochemistry.[22] Anti-cytokeratin (AE1/AE3, DAKO) and anti-vimentin (Vim3B4, DAKO) antibodies were used to exclude cores with questionable antigenicity from further analysis, and α-smooth muscle actin (SMA) (1A4, DAKO) and desmin (D33, DAKO) were used to identify cell types in the cancerous stroma. Dilutions for each antibody were 1:200 for cytokeratin, 1:200 for vimentin, 1:100 for SMA, 1:200 for desmin, and 1:10 000 for podoplanin.

Specificity of the immunohistochemical staining for podoplanin was confirmed by staining an in vitro grown cell line that was formalin fixed and paraffin embedded.[23] The cell line NIH3T3 was cultured and transfected with podoplanin gene using FuGENE6 (Roche, Tokyo, Japan) as previously described.[22] After the transfection, the cells were scraped, and the pellet was fixed in formalin and embedded in a paraffin block as an ordinary clinical tissue sample.[20] As a negative control, wild-type NIH3T3 cell line was identically processed. Four-micron thick sliced specimens from both the transfected cell line block and the wild-type cell line block were stained with podoplanin as described previously.

Analysis Using Conventional Pathology Sections

Consideration of tissue heterogeneity must be taken into account when analyzing TMAs. With markers that demonstrate remarkable tissue heterogeneity, staining with 2 to 3 different cores is frequently required.[24] To validate stromal podoplanin staining results seen in TMAs, we compared the immunohistochemical staining results between selected cores and the corresponding original whole tissue sections. Three each of positive and negative cases with podoplanin staining in the TMA were selected at random and compared with whole sections of the same specimens. The staining pattern was concordant between the TMA and the whole sections analyzed. To confirm if stromal podoplanin staining is unique to malignant processes, we also stained specimens from 6 inflammatory lung diseases including usual interstitial pneumonia, atelectasis, and organizing pneumonia, which have a combination of inflammatory cells, myofibroblastic proliferation, and collagen deposition.

Evaluation of Lymphatic Vessel Density in Relation to Podoplanin Expression

In a manner similar to the reported method to evaluate microvessel density,[25] 20 fields were selected in the areas with high number of lymphatic vessels, and lumens of lymphatic vessels were counted in the ×20 objective field (1.3 mm^2). Mean numbers of microlymphatic vessels were calculated and compared using *t* tests.

Scoring of Immunostaining Results in TMA

We scored immunohistochemical staining as previously described.[23] Specifically, the distribution score, which reflects the distribution of the positive signal among stromal cells, was scored as 0 (0%), 1 (1%–50%), or 2 (51%–100%) to reflect the percentage of positive staining among stromal cells seen in the same tissue core. The intensity score, intensity of the signal, was scored as 0 (no signal), 1 (weak), 2 (moderate), or 3 (marked). The sum of distribution and intensity scores (distribution score + intensity score; range, 0–5) was converted into total score (TS): TS = 0 (sum, 0), TS = 1 (sum, 2), TS = 2 (sum, 3), and TS = 3 (sum, 4 or 5). TS 0 and TS 1 were considered negative, whereas TS 2 and TS 3 were considered positive.[20,23] In case of discrepancy in scores between duplicated cores from the same patient, the higher score was assigned as the final score.

Statistical Analysis

Using the χ^2 test, we compared the positive and negative groups of podoplanin staining of multiple cancer TMA and lung cancer TMA on the basis of clinicopathologic factors that included age at diagnosis, sex, histologic type, pathologic stage, and TNM. When one arm of expected numbers was less than 5, Fisher exact test was applied. Survival analysis of lung cancer patients was performed using the log-rank test for comparing positive and negative groups of staining. Kaplan-Meier curves for the 2 groups were plotted based on overall survival. We accounted for clinical factors by fitting Cox proportional hazards models. The *P* value for the survival analysis corresponds to the log-rank test. *P* values were considered significant when they were less than .05.

RESULTS

The staining of podoplanin in transfected NIH3T3 showed specific membranous signal in approximately 10% to 20% of the cells (Figure 1, A), whereas wild-type NIH3T3 cells were negative (data not shown). Examining the staining in the reactive stroma in response to cancer, 43% of cores in multiple cancer TMA (Figure 1, B) and 33% of cores in lung cancer TMA were positive for

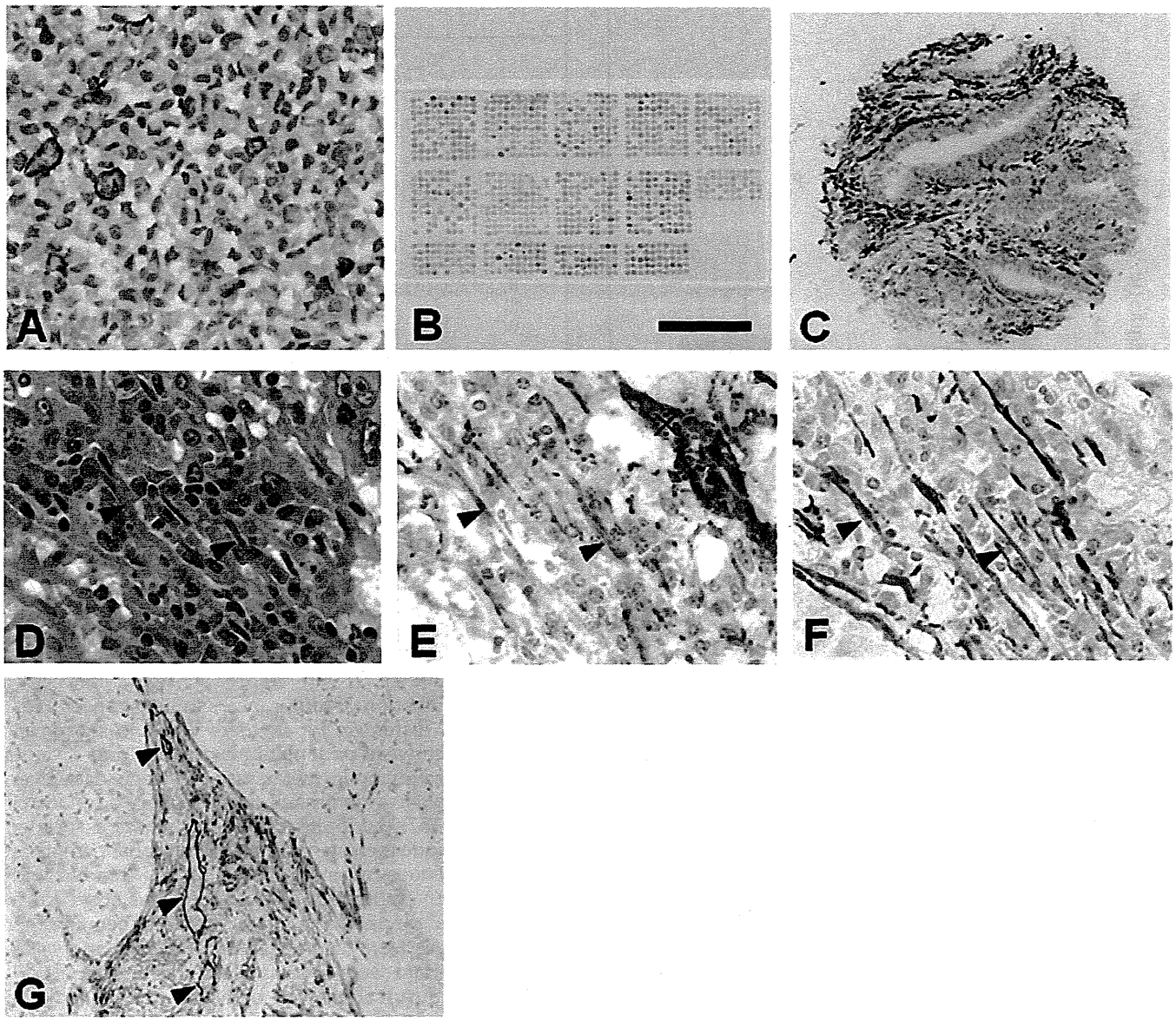

Figure 1. *Immunohistochemical detection of podoplanin in cancerous stroma. A, Validation of podoplanin immunohistochemical staining using podoplanin transfected NIH3T3 cells. Paraffin-embedded cells demonstrate membranous signals in 10% to 20% of cells (original magnification ×400). B and C, Images of a tissue microarray. B, Overview of multiple cancer tissue microarray with podoplanin staining. Each group has either 100 or 50 cores from 1 cancer type. A total of 1150 cases from 14 different cancer types are included (scale bar = 1 cm). C, Representative core positive for anti-podoplanin staining in cancerous stromal cells (diameter of the core is 0.6 mm). D through F, High-power view of cancerous stroma stained with hematoxylin-eosin (D), anti-podoplanin (E), and anti–α-smooth muscle actin (F) using consecutive sections (original magnifications ×400 [D through F]). Arrowheads indicate nonneoplastic spindle cells seen in the cancerous stroma. Identical cells are positive for podoplanin and α-smooth muscle actin. Spindle cells positive for podoplanin were considered as myofibroblasts based on the staining patterns and morphology (asterisk in E, lymphatic vessel stained with podoplanin). G, Cancerous stromal cells and lymphatic vessels (arrowheads) are positive for podoplanin (original magnification ×100). Lymphatic vessels stained more intensely with podoplanin than did stromal spindle cells.*

podoplanin (Figure 1, C). Stromal cells (Figure 1, D) coexpressed podoplanin (Figure 1, E) and SMA (Figure 1, F) but were negative for desmin, confirming them as myofibroblasts. Inflammatory cells, mainly lymphocytes and macrophages, present in the same stroma were negative for podoplanin. Lymphatic vessels stained more intensely with podoplanin than did podoplanin-positive stroma (Figure 1, E and G). The mean numbers of lymphatic vessels were significantly higher in the stroma with podoplanin-positive expression (5.2 ± 1.23) than in stroma with podoplanin-negative expression (1.9 ± 1.12) (P = .01) (Figure 2).

A total of 1152 patients had clinical and pathologic information. Of 1152 cases, 126 cases were excluded as inadequate for scoring. We applied a criteria that tissue cores that were immunohistochemically negative for both cytokeratin and vimentin would be excluded from analysis based on the assumption that most carcinomas should demonstrate pancytokeratin staining, and most interstitial cells should be reactive for vimentin. By this method, 3 cores were excluded from the experiment. An additional 145 cases were also excluded due to absence of cancerous stromal tissue in the core by hematoxylin-eosin light microscopic examination. Most renal cell carcinomas